Journal Pre-proof

Glycyrrhiza glabra (Licorice) root extract attenuates doxorubicin-induced cardiotoxicity via alleviating oxidative stress and stabilising the cardiac health in H9c2 cardiomyocytes

Shishir Upadhyay, Anil K. Mantha, Monisha Dhiman

PII: S0378-8741(19)34055-3

DOI: https://doi.org/10.1016/j.jep.2020.112690

Reference: JEP 112690

To appear in: *Journal of Ethnopharmacology*

Received Date: 9 October 2019

Revised Date: 19 February 2020

Accepted Date: 19 February 2020

Please cite this article as: Upadhyay, S., Mantha, A.K., Dhiman, M., *Glycyrrhiza glabra* (Licorice) root extract attenuates doxorubicin-induced cardiotoxicity via alleviating oxidative stress and stabilising the cardiac health in H9c2 cardiomyocytes, *Journal of Ethnopharmacology* (2020), doi: https://doi.org/10.1016/j.jep.2020.112690.

Glycyrrhiza glabra (Licorice) Root Extract Attenuates Doxorubicin-Induced Cardiotoxicity via Alleviating Oxidative Stress and Stabilising the Cardiac Health in H9c2 Cardiomyocytes

Shishir Upadhyay[1], Anil K. Mantha[1], Monisha Dhiman[2 *]

[1] Department of Zoology, School of Basic and Applied Sciences, Central University of Punjab, Bathinda, 151001, Punjab, India

[2] Department of Microbiology, School of Basic and Applied Sciences, Central University of Punjab, Bathinda, 151001, Punjab, India

[*] Corresponding author

Address for Communication:

Dr. Monisha Dhiman, Ph.D.
Associate Professor
Department of Microbiology
School of Basic and Applied Sciences
Central University of Punjab, Bathinda
Punjab, Pin Code: 151001
India
Email: monisha.dhiman@cup.edu.in
Phone: +91-164-2864260

Orcid ID: 0000-0001-5923-3384

Contribution of the Authors:
Conceived and designed the experiments: SU, AKM and MD
Performed the experiments: SU
Analyzed the data and compiled manuscript: SU, AKM and MD
Contributed reagents/materials/analysis tools: MD and AKM

Abstract

Ethnopharmacological relevance: Doxorubicin (DOX) is an effective anti-neoplastic drug, however; it has downside effects on cardiac health and other vital organs. The herbal remedies used in day to day life may have a beneficial effect without disturbing the health of the vital organs. *Glycyrrhiza glabra L*. is a ligneous perennial shrub belonging to Leguminosae/ Fabaceae/ Papilionaceae family growing in Mediterranean region and Asia and widespread in Turkey, Italy, Spain, Russia, Syria, Iran, China, India and Israel. Commonly known as mulaithi in north India, *G. glabra* has glycyrrhizin, glycyrrhetic acid, isoliquiritin, isoflavones, etc., which have been reported for several pharmacological activities such as anti-demulcent, anti-ulcer, anti-cancer, anti-inflammatory and anti-diabetic.

Aim of the study: The objective of the present study is to investigate the interaction between the molecular factors like PPAR-α/γ and SIRT-1 during cardiac failure arbitrated by DOX under *in vitro* conditions and role of *Glycyrrhiza glabra* (*Gg*) root extract in alleviating these affects.

Materials and Methods: In the present study, we have examined the DOX induced responses in H9c2 cardiomyocytes and investigated the role of phytochemical *Glycyrrhiza glabra* in modulating these affects. MTT assay was done to evaluate the cell viability, Reactive Oxygen Species (ROS)/Reactive Nitrogen Species (RNS) levels, mitochondrial ROS, mitochondrial membrane potential was estimated using fluorescent probes. The oxidative stress in terms of protein carbonylation, lipid peroxidation and DNA damage was detected via spectrophotometric methods and immune-fluorescence imaging. The cardiac markers and interaction between SIRT-1 and PPAR-α/γ was measured using Real-Time PCR, Western Blotting and Co-immunoprecipitation based studies.

Results: The *Glycyrrhiza glabra* (*Gg*) extracts maintained the membrane integrity and improved the lipid homeostasis and stabilized cytoskeletal element actin. *Gg* phytoextracts attenuated aggravated ROS level, repaired the antioxidant status and consequently, assisted in repairing the DNA damage and mitochondrial function. Further, the expression of hypertrophic markers in the DOX treated cardiomyocytes reconciled the expression factors both at the transcriptional and translational levels after *Gg* treatment. SIRT-1 mediated pathway and its downstream activator PPAR factors are significant in maintaining the cellular functions. It was observed that the *Gg* extract allows regaining the nuclear SIRT-1 and PPAR-γ level which was otherwise reduced with DOX treatment in H9c2 cardiomyocytes.

The co-immunoprecipitation (Co-IP) documented that SIRT-1 interacts with PPAR-α in the untreated control H9c2 cardiomyocytes whereas DOX treatment interferes and diminishes this interaction however the *Gg* treatment maintains this interaction. Knocking down SIRT-1 also downregulated expression of PPAR-α and PPAR-γ in DOX treated cells and *Gg* treatment was able to enhance the expression of PPAR-α and PPAR-γ in SIRT-1 knocked down cardiomyocytes.

Conclusions: The antioxidant property of *Gg* defend the cardiac cells against the DOX induced toxicity via; 1) reducing the oxidative stress, 2) maintaining the mitochondrial functions, 3) regulating lipid homeostasis and cardiac metabolism through SIRT-1 pathway and 4) conserving the cardiac hypertrophy and hence preserving the cardiomyocytes health. Therefore, *Gg* can be recommended as a healthier supplement with DOX towards cancer therapeutics associated cardiotoxicity.

Keywords: Cardiac Metabolism; Cardiotoxicity; Doxorubicin; Mitochondrial Dysfunction; Oxidative Stress.

Graphical Abstract:

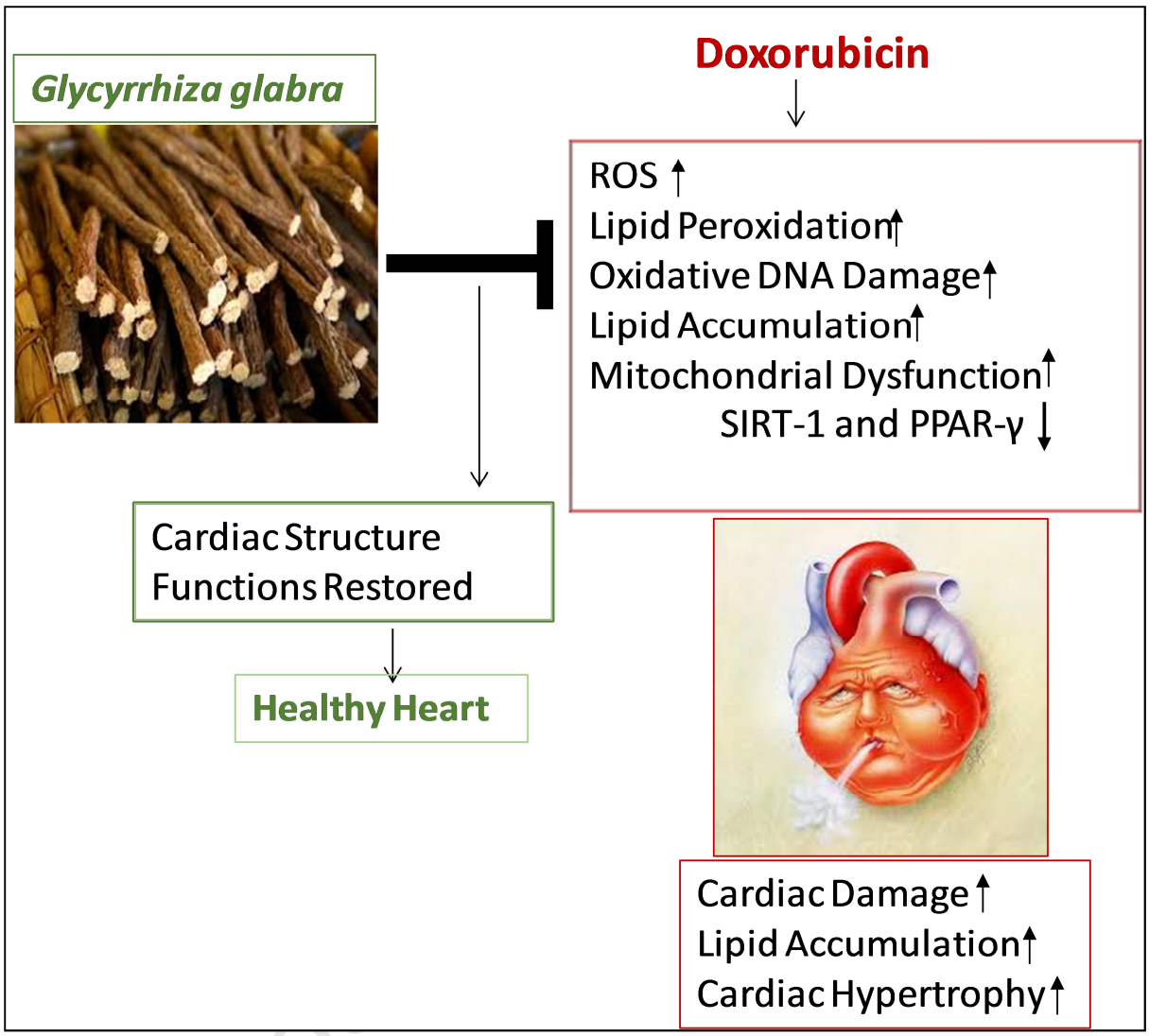

Introduction

Doxorubicin (DOX), an anti-neoplastic drug reported to have cardiac associated side effects such as cardiomyopathy and ischemia/perfusion. The effects can be acute to chronic depending on the susceptibilty and dose of the drug employed. DOX acts as an oxidant and prompts high reactive oxygen species (ROS) levels which damage cellular lipids, proteins, or DNA; hence, hindering their regular functions, a phenomenon implicated very well in many human diseases (Montaigne *et al.,* 2012). A highly oxidative metabolic environment and relatively poor antioxidant defense system predisposes the cardiac cells to free radical damage (Montaigne *et al.,* 2012). The cardiac cells require a continuous form of energy for their functioning and collaborates with more number of mitochondria to achieve their energy requirement (Dolinsky, 2017). DOX is also responsible for mitochondrial and metabolic dysfunctioning of the cardiac cells including glucose oxidation, lipid metabolism (Strigun *et al.,* 2011 & Hrelia *et al.,* 2002) which can further inhibit the functions of several transcription factors (TFs) such as Sirtuins (SIRT) (Franceschelli *et al.,* 2016).

SIRT-1 further alters the activity of downstream molecules such as Peroxisomes Proliferator-Activated Receptors (PPAR-α/γ), which are important during cardiac hypertrophy (Hsu *et al.,* 2010). The protective role of SIRT-1 in cardiomyocyte injury induced by DOX through stimulating the PPAR-α/γ during stress has been investigated under *in vivo* and *in vitro* conditions (Han *et al.,* 2010 & Oka *et al.,* 2012). The nuclear PPAR-α expression has been reported to be reduced in the hypertrophic mouse model and found to be deactivated during the treatment with an α-adrenergic agonist (e.g., phenylephrine) to the neonatal cardiac myocytes (Barger *et al.,* 2000). PPAR-α binds and recruits SIRT-1 to the estrogen related receptors response element (ERRE), which further suppresses the ERR target genes such as those participating in mitochondrial function (Oka *et al.,* 2012). PPAR-α can also attenuate the cardiac hypertrophy by inhibiting the inflammatory pathways through NF-κB (Planavila *et al.,* 2005). Thus, absence of either SIRT-1 or PPAR-α/γ can cause the cardiac dysfunction, whereas their simultaneous up-regulation enhances cardiac functions. Besides SIRTs and PPARs, other essential elements that are crucial for the heart functioning include Myosin Light Chain 2 (MLC-2v) and GATA (namely GATA-4 & GATA-6) which are also considered as hypertrophic markers. Numerous other hypertrophic markers (such as ANP, BNP, MHC, and Troponin I) are also reported to get modulated during the DOX

treatment. Emerging evidences show that the PPAR signalling pathways play critical role in the regulation of these factors within the cardiovascular system.

Glycyrrhiza glabra (*Gg*) is commonly referred as Licorice, is a perennial legume, native to the various regions such as Middle East, southern Europe, and India. It is used in many systems of medicines including Unani, Ayurveda. Homeopathy, Chinese and Siddha to cure various types of complications like hepatitis, ulcers, pulmonary, skin diseases. Ethnically it is used for the treatment of chronic viral hepatitis in Japan, tuberculosis in China, and peptic ulcers and mouth ulcers in many other parts of the world (Dhingra *et al*., 2004). Licorice was known in Chinese medicine as early as 2800 B.C. In Tibet, it was considered a classical medicine. The use of licorice preparations to alleviate throat and bronchial infections was known for more than 2000 years. Its major phytoconstituents are glycyrrhizin, glycyrrhizinic acid, glabrin A&B, glycyrrhetol, glabrolide, isoglabrolide, isoflavones, coumarins, triterpene sterols. It is well recognised **a**nti-inflammatory, anti-artherogenic and hypocholestremic plant (Ammar *et al.,* 2012). Additionally, its antioxidant property can protect the heart from myocardial injury and flavonoids present in the root extracts confer anti-inflammatory property which can improve the cardiac performance (Visavadiya *et al.*, 2009).

The present study was conducted to investigate whether the aqueous extract of *Gg* roots counteract the toxicity of DOX on cardiac cells and modulate the expression of effective molecular factors. The effect of phytoextracts in the manifestation of signaling pathways involving SIRT-1, PPAR-α/γ as well as oxidant/antioxidant enzymes (NOS2, SOD1 and SOD2) in DOX-induced cytotoxicity using H9c2 cardiomyocytes was assessed. Furthermore, experiments were also performed to examine whether loss of SIRT1 (RNAi mediated) has any direct impact on PPAR-α/-γ expression and hypertrophy in DOX treated cardiomyocytes to implicate DOX-mediated cardiotoxicity and phytochemical *Gg*- mediated activation of cellular mechanisms via SIRT-1 and PPARs.

Materials and Methods

Culturing of Cardiomyocytes

H9c2 myoblasts are well reported cell model used as an alternative for cardiomyocytes (Liu *et al.,* 2016). Rat cardiomyocytes (H9c2) cells used in this study were procured from NCCS, Pune. The cells were cultured in DMEM supplemented with 10% heat-inactivated FBS, 100µg/ml streptomycin, and 100units/ml penicillin at 37°C in a

humidified atmosphere (5% CO_2; 95% O_2). The H9c2 cells were sub-cultured at 80-90% confluent stage, and were used for experimental design. The FBS starved cells were used for all the treatment used in present study.

Preparation of Plant Extract

The *Glycyrrhiza glabra* roots were collected from the herbal garden of Dr. Y. S. Parmar University of Horticulture & Forestry, Solan (HP) and were identified and authenticated in the Department of Forest Plant Products. *Gg* root was crushed into fine powder and dissolved in 30 ml distilled H_2O for overnight at 50°C on a magnetic stirrer. The solution was filtered with Whatmann filter paper and centrifuged for 30 min at 10,000 rpm. The supernatant was dried in rota-evaporator kept at 40°C. The extract was dissolved in PBS and stored at 4°C until further use (Al-Obaidi, 2013).

Assessment of Cell Viability in the Presence of *Gg* Root Extract

The H9c2 cells were incubated with DOX (1-5µM) (MP Biomedicals) in FBS free DMEM media. The H9c2 cells were treated with the *Gg* extracts at different concentrations (20 - 200µg/ml) with selected dose of DOX in 96 well plates. Cell viability was determined using a modified 3-(4.5-dimethylthiazol-2-yl)-2.5-diphenyltetrazolium (MTT) assay. Briefly, MTT solution was added to the wells at a final concentration of 0.5 mg/ml. After 4 hr, the formazan crystals were dissolved in DMSO and the absorbance was recorded at 570 nm using a microplate reader (Synergy H1) (Upadhyay *et al.,* 2019). The selected concentration of *Gg* with DOX was also used to treat the breast cancer MDA-MB cells.

LDH Assay

LDH (Lactate dehydrogenase) released from the cytosol of damaged cells considered as indicator of membrane disruption during cell's injury. LDH cytotoxicity detection kit (Cayman) was used as per the manufacturer's protocol. LDH released into the extracellular medium of cells treated with different concentrations of free DOX, were expressed as a percentage of the total LDH activity in the H9c2 cells (Dhiman *et al.,* 2013).

Analysis of the Cell Morphology

H9c2 cells were seeded at a density of $2.5X10^5$ cells/well in 6-well plates. Cells were then treated with DOX (5µM) and DOX + *Gg* for 24 hr. Cells were stained with Haematoxylin stain and morphology was examined under the microscope (Olympus

FX100). $2X10^4$ cells were seeded on cover slips and treated with DOX and DOX + *Gg* for 24 hr. H9c2 cells were fixed in 2% paraformaldehyde (PFA) and permeabilized in 0.1% Triton X-100. Immunostaining was performed by using phalloidin. The cells were counterstained with DAPI for nuclear staining. Images were analyzed using Olympus SV-1200 Laser Scanning Confocal Microscope.

Oil Red O Staining

Oil Red O (ORO) was employed to determine the neutral lipid accumulation in DOX, DOX + *Gg* treated cells. Briefly, cells were cultured in 6-well plates at a density of $2.5X10^5$ cells/well, and after indicated treatments, cells were rinsed with 60% isopropanol and dipped in ORO working staining solution at RT for 15 min and rinsed thrice in distilled H_2O. Images were obtained using an Olympus inverted Microscope (Ma *et al.*,2012).

Assessment of Oxidative Stress in H9c2 Cells

Oxidative stress in the form of intracellular ROS was determined via the NBT, DHE, H_2DCFDA assay. After the treatment, H9c2 cells were washed with PBS, incubated for 30 min with NBT with final concentration (0.1mg/ml), and again washed with PBS. The treated cells were trypsinized and the relative absorbance of untreated, DOX-treated, DOX+ *Gg* extract- treated cells was measured at 620 nm with Biotek microplate reader (Dhiman and Garg, 2011).

The H9c2 cells were seeded into 96 well plates and incubated with H_2DCFDA (2 µM) in incubator for half an hour. The H_2DCFDA was aspirated off and washed with PBS twice. The cells were co-treated with DOX and *Gg* for 24 hr. The reading was taken at Ex/Em 492/517 nm. The cells were incubated with other probes such as DHE for 30 min and washed with PBS and reading was taken at Ex/Em (518⁄605 nm) (Gupta *et al.,* 2009).

DOX Induced DNA Damage

Cells ($2X10^4$) were seeded on cover slips and treated with DOX and DOX +*Gg* for 24 hr. DNA damage detection with 8-Oxo-dG antibody was performed as per manufacturer's protocols (Trevigen). The cells were fixed in chilled methanol acetone (1:1) at -20°C for 15 minutes and further incubated in 0.05N HCl for 5 min followed by RNAase containing solution (150mM NaCl, 15mM sodium citrate) for 1 hr at 37°C. The DNA was denatured *in situ* with solution (0.15N NaOH in 70% ethanol) for 5 min. The cells were washed sequentially in 70% ethanol containing 4% v/v formaldehyde, 50% and 35% ethanol and incubated in 5µg/ml proteinase K in 20mM Tris, 1mM EDTA, pH 7.5 for 10 min at 37°C.

The non-specific sites were blocked with 5% BSA at 37°C for 1 hr and incubated with anti-8-Oxo-dG antibody (1:250 diluted) in 1X PBS containing 1% BSA, 0.01% Tween 20 at 4°C in a humidified chamber. After washing the cells were incubated with Alexa flour-488 tagged secondary antibody at 37°C for 1 hr and counterstained with Hoescht 33342. The images were analyzed using Olympus SV-1200 Laser Scanning Confocal Microscope (CIL, CUPB).

Mitochondrial ROS and Potential (MTP)

H9c2 cells were treated with DOX in the presence and in absence of *Gg* and incubated with 200 nM MitoTracker Red and 5 μM MitoSOX Red for 30 min, cells were then washed thrice with PBS. Subsequently, the cells were analyzed using Olympus SV-1200 Laser Scanning Confocal Microscope (Sarkar, *et al.*, 2017).

5,5',6,6'-tetrachloro-1,1',3,3'-tetraethylbenzimidazolylcarbocyanine iodide probe (JC-1, Molecular probes) was employed to determine the mitochondrial transmembrane potential (MTP) effect of DOX and DOX + *Gg* treatment. Treated cells were incubated with an equal volume of JC-1 staining solution (5 μg/ml) at 37°C for 20 min in the dark and rinsed with PBS following the manufacturer's instructions. MTP was analysed by determining the relative amounts of mitochondrial JC-1 monomers (green fluorescence, meaning lower MTP) and aggregates (red fluorescence, meaning higher MTP) using a fluorometer (Synergy H1). Mitochondrial depolarization could be indicated by an increase in the green/red fluorescence intensity ratio (Gupta *et al.*, 2009).

RNA Isolation and Real-Time Polymerase Chain Reaction

Total RNA was isolated from DOX and DOX + *Gg* treated H9c2 cardiomyocytes using PureZOL (Bio-Rad), followed the manufacturer's instructions. It was used to make cDNA by using reverse transcriptase with primers as described by the manufacturer (Thermo Scientific). Real-time quantitative RT-PCR was performed using Maxima SYBR green/ROX qPCR master mix (Thermo Scientific). Programmed the thermal cycler with holding stage {95°C (10 min)}, cycling stage {denaturation temp 95°C (15 min), annealing temperature 55°C (1 min), extension temperature 72°C (1 min)}, melt curve stage {60°C (30 min) 95°C (15 min)} with SYBR Premix ExTaq (1 μL of cDNA, 12.5 μL of SYBR Universal PCR Master Mix (BioRad), 250 nM probes, and 900 nM primers) **(Table 1).** The amount of mRNA was normalized to GAPDH mRNA. By using the comparative ($2^{-\Delta CT}$) method, calculated the mRNA expressions of treated H9c2 cells (Dhiman and Garg, 2011).

Western Blotting

Protein expression was evaluated by Western blotting and quantified with densitometry. DOX and DOX + *Gg* treated H9c2 cells were trypsinized and pellets were resuspended in lysis buffer (20 mM HEPES pH 7.5, 20% glycerol, 150 mM NaCl, 1 mM EDTA, 1 mM EGTA, 5 mM DTT, 100 µM PMSF, and 1X protease inhibitor cocktail). Bradford method was used to measure protein contents utilising BSA as a standard. Equivalent amount (50 µg) of proteins were mixed with loading buffer (2X) supplemented with β-mercaptoethanol and boiled at 95°C for 5 min. Proteins were then resolved by electrophoresis in 10-12% SDS-polyacrylamide gels (SDS-PAGE) and blotted on to Nitrocellulose (NC) membranes. After blocking with 5% milk in TBST [50 mM Tris-HCl (pH 8), 154 mM NaCl, and 0.1% Tween20] for 2 hr at room temperature, the membranes were incubated overnight at 4°C with specific antibodies such as rabbit polyclonal anti-SIRT-1, anti-PPARα, anti-PPARγ, NOS2, SOD1&2, anti-MLC-2v, anti-MHC, anti-troponin-I and mouse monoclonal β-actin (Sarkar, *et al.*, 2017).

Cytosolic extracts were obtained with hypotonic shock method, the cell pellets were treated with 100 µl of buffer A (20 mM HEPES, 20% Glycerol, 10 mM NaCl, 1.5 mM $MgCl_2$, 0.2 mM EDTA, 0.1% Triton X-100, 1 mM DTT, 100 mM PMSF, Protease Inhibitors Cocktail) on ice for 15 min and centrifuged at low speed. The supernatant (cytosolic extract) was stored at -20°C until further use. Nuclear extract was prepared by treating the cell pellet with hypertonic solution (20 mM HEPES, 20% Glycerol, 500 mM NaCl, 1.5 mM $MgCl_2$, 0.2 mM EDTA, 0.1% Triton X-100, DTT, PMSF, Protease Inhibitors Cocktail) with intermittent tapping for 1 hr at 4°C, followed by centrifugation at high 14,000 rpm. Western blot analysis was performed using antibody against SIRT-1, PPAR-α, PPAR-γ with housekeeping protein (β-Actin) and PCNA for cytoplasmic and nuclear, respectively, as an internal control. Specific signals were visualized using the BioRad gel doc system (Levrand *et al.*, 2005).

Co-immunoprecipitation

For investigating the PPAR-α and PPAR-γ and SIRT-1 interactions, co-immunoprecipitation was performed according to the manufacturer instructions with slight modification. Briefly, H9c2 cardiomyocyte lysates were added with isotype of antibody to make precleared lysates. The SureBeads (BioRad) with protein A/G were chosen according to antibody (species specific and polyclonal/monoclonal specific). The SureBeads were magnetised and washed with PBST (pH-7.4) thrice. Antibody (PPAR-α and PPAR-γ 5µg in 200 µl PBST) was added and beads were re-suspended. The vials were kept at 4°C for 1 hr at slow rotation. An amount of 200 µg of protein was added to the beads and incubated

overnight for continuous rotation. The vials were centrifuged at low speed (2500 rpm) for 90 seconds. The pelleted samples were then mixed with Lammelli sample buffer and incubated for 10 min at 70°C. Magnetised beads and eluent was transferred to new vial and eluent was boiled at 95°C for 5 min and loaded onto SDS-PAGE gel and followed by Western blot with SIRT-1 antibody as described earlier.

siRNA Transfection

The H9c2 cardiomyocytes were seeded into six well plates at 30-50% confluence. The specific oligonucleotide sequences negative control (NC) and siRNA SIRT-1 **(Table 2),** were synthesised by Eurogentec. Two solutions were prepared solution A (solution 1 containing 4.5ml OptiMEM media and siRNA 9 µl (100nM); and solution 2 containing 4.5ml Media and 100 µl (Lipofectamine) and solution B (solution 1 containing 4.5ml OptiMEM media + control siRNA 9µl (100 nM); solution 2 containing 4.5 ml Media and 100 µl Lipofectamine). After 6 hr, the media was replaced with incomplete media containing DOX treatment. After 24 hr, the H9c2 cells were scrapped with lysis buffer (mentioned above) and lysates were prepared and stored at -20°C till further experiments.

Statistical Analysis

Statistical analyses were performed using unpaired Student's t-tests with the microsoft excel. Data is represented as (Mean ±SEM) where n=3. Statistical significance was accepted at $P < 0.05$.

Results

Effect of Doxorubicin on Viability of H9c2 Cardiomyocytes

We first examined the response of the DOX on H9c2 cells survival at 24 hr **(Fig. 1A).** The results showed that the cell viability was decreased by 42% with 5 µM of DOX concentration when compared to untreated control cells (57.5 ± 7.07 vs. 100). Whereas, 1,2,3 & 4 µM of DOX concentration reduced the cell viability by 19%, 29 %, 30% and 27%, respectively (81 ± 2.4, 71 ± 9.5, 70 ± 7.8, 73.4 ± 7 vs. 100, respectively). In further experiments, 5 µM DOX concentration was used as a treatment dose which is also used in previous reports (Liu *et al.,* 2016).

Effect of Root Extract of *Gg* against DOX induced Cardiotoxic Effects

To weaken the insulting effect of DOX on H9c2 cardiomyocytes, the cells were treated with different concentrations (20 µg/ml to 200 µg/ml) of aqueous extract of *Gg* before

DOX (5 µM) treatment. We observed that aqueous extract with chosen concentration (40 µg/ml) showed significant increase in H9c2 cell survival by 24% when compared to DOX treated cells (83±10.08 vs. 59 ±8.12) ($P<0.05$) **(Fig. 1B).**

In order to verify that the aqueous extract of *Gg* are not interfering in the anti-cancer activity of DOX, we used MDA-MB Breast cancer cell line. MTT assay was performed at 24 hr after incubation with selective dose of *Gg* extract on DOX treated MDA-MB cell line. There was a significant decrease of 60% (34±5.6 vs 100) in the cell viability as compared to untreated control H9c2 cells, suggesting that *Gg* extract do not interfere with the DOX induced toxicity in cancer cells (101±2.2 vs 100) **(Fig. 1C)**.

Effect of DOX on Cell Morphology and Cell Integrity

Cell morphology is an important parameter to evaluate the effect of any treatment on cells. Haematoxylin staining was used to study the morphological characteristics of DOX treated H9c2 cardiomyocytes in the presence of *Gg* **(Fig. 2A**). The cells appeared enlarged and their morphology was prominently altered. In addition confocal Fluorescence microscopy was performed to detect the F-actin with phalloidin to uncover the morphological changes in DOX and DOX + *Gg* treated H9c2 cardiomyocytes. F-actin was disintegrated in the presence of DOX while the *Gg* helped in maintaining the cytoskeleton hence conserving the structure and morphology of the cells **(Fig. 2B-Panel 1-3)**.

Lactate dehydrogenase (LDH) is another important marker of cell damage**.** The membrane integrity of cardiomyocytes upon treatment with DOX (5µM) and DOX (5µM) + *Gg* (40µg) were determined by LDH release assay. In the presence of DOX alone, the level of LDH release in culture supernatant increased to about 3 fold (245.7 ± 0.02 Vs 100 ± 0.02) as compared to untreated control cardiomyocytes. While the treatment of *Gg* along with DOX reduced the LDH release (179 ± 0.04 Vs 245.7±0.02) by 73% **(Fig. 2B).**

Effect of DOX on Oxidative Stress

In order to assess the ROS level in aqueous *Gg*, co-treated H9c2 cardiomyocytes with selected dose (40µg/ml), before DOX treatment. DOX induces cardiotoxicity through ROS generation, there was a significant increase (348.43± 71.55 vs 100±7.4) in the ROS level in H9c2 cardiomyocytes when treated with DOX alone. The level of total ROS was significantly reduced in DOX + *Gg* treated cells when compared with DOX treatment (252± 31 vs 348.43 ± 71.55) **(Fig. 3A)**.

Fluorescence based assays were performed to assess the ROS level using H_2DCFDA and DHE probes. The oxidative ROS levels increased up to five folds (473.12 ±91 vs 100) in the cells treated with DOX. Whereas *Gg* extract decreased the ROS level by three folds (183.3± 38 vs 473.12 ±91) **(Fig. 3B).** The free intracellular superoxide level was analysed by another sensitive fluorescent dye dihydroethidium or hydroethidine (DHE). The intracellular superoxide level in DOX treated cells increased up to 3 folds (271.8±3.8 vs 100 ±2.9), whereas the *Gg* extract reduced the superoxide level by 62% **(Fig. 3C).** Overall results suggest the free radical scavenging property of *Gg* aqueous extract.

Effects of DOX on Mitochondrial ROS and Membrane Potential

To evaluate the contribution of mitochondrial ROS and role of *Gg* extract towards mitochondrial membrane potential in DOX treated H9c2 cells, Mitosox assay was performed. Confocal microscopic imaging showed increase in mitochondrial fluorescence intensity of MitoSOX (green) in H9c2 cells treated with DOX. In the presence of *Gg*, the DOX treated H9c2 cardiomyocytes showed decrease in fluorescence intensity when compared with DOX treated H9c2 cells **(Fig 4A-Panel 2).** The mitochondria was stained with mitotracker **(Fig 4A- Panel 3).**

The mitochondrial membrane potential (ΔΨm) is a sensitive parameter to detect mitochondrial damage. The carbocyanine dye JC-1 dye was used to interrogate the mitochondrial health on the basis of dual wavelength emission in H9c2 cardiomyocytes. According to mitochondrial health, the color shifted from orange red aggregates (healthy cells) to green coloured monomer (apoptotic marker) upon the treatment of DOX (5µM), while the orange red aggregates occurred in normal untreated H9c2 cells. When cardiomyocytes were incubated with *Gg* with toxic concentration (5 µM) of DOX for 24 hr, ΔΨm depolarization (red to green ratio) of cardiomyocytes was maintained as normal cells **(Fig 4B).**

Evaluation of DOX Induced DNA Damage and Apoptosis

8-oxo-dG is a parameter of DNA damage induced by oxidized derivative of deoxyguanosine. The 8-oxo-dG, antibody was used to measure DNA damage in H9c2 cells treated with DOX and DOX + *Gg*. In control H9c2 cells, 8-oxo-dG staining was found to be basal level (not observed) indicating undamaged DNA, whereas DOX treated H9c2 cells showed higher fluorescence depicting high DNA damage **(Fig 5A-Panel 2).**

Effect of DOX on Antioxidant Enzymes

The ROS generation upon DOX treatment indicated its influence on antioxidant defense. The SOD1 and SOD2 expression was found to be reduced to 40% and 80% respectively, while the NOS2 is increased by 2 fold. Results clearly advocate that DOX action is mediated through oxidative stress, whereas, the Gg along with DOX tried to recover the normal condition against DOX induced oxidative stress **(Fig. 6A-D).**

Effect of DOX on Metabolic Regulators

Oil red O is a fat soluble diazol dye which indicates the lipid homoeostasis in cells. Oil red O shows more solubility in neutral fats as compared to alcohol, in which dye has been prepared. Lipid metabolism was disrupted by DOX as indicated in **Fig. 7A**. Oil red staining showed significant deposition of fat droplets of H9c2 incubation with DOX (5µM) whereas in *Gg* + DOX treated H9c2 cells, showed depletion in lipid accumulation **(Fig. 7A)** suggesting that *Gg* maintains the cell morphology and structure which will ultimately protect the cardiac tissue too.

Further, insufficient levels of either SIRT-1 or PPAR-α can attenuate mitochondrial dysfunction, whereas their simultaneous up-regulation has the opposite effect. In the presence of DOX, some important metabolic regulating proteins such as SIRT-1 and PPARs (PPAR α and γ), gets altered. SIRT-1 and PPAR-γ expression was decreased by 30 % & 20%, respectively, in the presence of DOX, while the PPAR α expression did not get much influenced. Whereas, in the presence of *Gg* alongwith DOX, the expression of SIRT-1 and PPAR-γ was found to be improved, while the level of PPAR α showed same expression (**Fig. 7B** & **C**). The mRNA level of PPAR α and SIRT1 was found to be significantly reduced when treated with DOX while the mRNA levels showed an increment of ~2 fold in DOX + *Gg* treated cells. The treatment of *Gg* solely increased the mRNA levels of PPAR-α and PPAR-γ (**Fig. 7D**).

In addition, we found that in the nuclear extracts of H9c2 cells the level of SIRT-1 and PPAR γ depleted to significant level in the nucleus when treated with DOX, whereas *Gg* might be involved in nuclear localisation of protein of SIRT-1, and PPARγ **(Fig 8A-D)**. It is not clear, how DOX halts the protein to migrate from cytoplasm to nucleus. In the cytosolic fraction the SIRT-1 and PPAR γ levels were reduced in the cytosol when treated with DOX alone (**Fig 8E-H**) and DOX+*Gg* treatment improved their levels in the cytoplasmic extracts. The PPAR α level was increased in DOX treated cytoplamic extracts whereas the DOX+*Gg* treatment normalised the PPAR α expression similar to the untreated controls (**Fig. 8E-H**).

Effect of DOX on Hypertrophic Markers

The cytoskeleton proteins form the basis of cross-bridge cyclin kinetics, and muscle contraction. For instance, a loss of Myosin Light Chain (MLC-2v) phosphorylation can directly lead to the pathogenesis of human dilated cardiomyopathy. DOX (5 µM) Treatment of increased the protein levels of MHC and troponin-I whereas Gg co-treatment with DOX reduced their levels **(Fig 9A-D).**

The mRNA levels of the hypertrophic markers MLC-2v, ANP, BNP, GATA-4 and GATA-6 were increased by ~2fold, ~3.5fold, ~1fold, ~.5fold, ~1fold (depicted in Log_2 scale) respectively in DOX treated H9c2 cells **(Fig 9)** while the co treatment of *Gg* along with DOX reduced the transcriptional level of ANP and MLC2v, whereas no much effect was seen on BNP, GATA-4 and GATA-6 levels.

Co-immunoprecipitation with PPAR-α and PPAR-γ with SIRT-1

To see the physical interaction between SIRT-1 and PPARs, co-immunoprecipitation was performed. The Co-IP and Western blotting showed that PPAR-α and PPAR-γ are potential partners of SIRT-1. The total cell lysate were co-immunoprecipitated with PPAR-α and PPAR-γ antibodies and Western blotting was performed with SIRT-1 antibody and using β-actin as loading control. The results showed that the level of SIRT-1 has a strong interaction with PPAR-α in untreated control immunoprecipitated samples where as SIRT-1 level was reduced in DOX treated H9c2 cardiomyocyte immunoprecipitated samples as compared to untreated control. However, the H9c2 cardiomyocyte, when treated with *Gg* along with DOX reconciled the interaction of SIRT-1 and PPAR-α **(Fig 10A).** The protein samples when immunoprecipitated with PPAR-γ, the SIRT-1 levels on the blot indicated that interaction with the PPAR-γ in both DOX treated and untreated H9c2 cardiomyocytes. However, when treated with *Gg* along with DOX, interactions get disappeared, a clear reason/explanation have to be investigated further **(Fig 10B).**

Search Tool for the Retrieval of Interacting Genes/Proteins (STRING) is a biological database and to predict the protein–protein interactions (https://string-db.org). *In silico* protein-protein interaction analysis was done to elucidate the PPAR α and PPAR γ interaction with SIRT-1 in normal cellular condition **(Fig 10C).** In this prediction it was calculated that the binding score with PPAR-γ (score: 0.481) PPAR-α (score: 0.420) with SIRT-1, indicated that moderate interaction was predicted on the basis of previously reported data **(Fig. 10C)** (Sarkar *et al.,* 2017).

siRNA Studies to Correlate the Interaction Between SIRT-1 and PPARs

It is reported that PPAR γ binds with SIRT-1 and influence the activity of each other, forming a negative feedback and self-regulation loop (Han *et al.,* 2010). Considering the regulatory role of SIRT-1 on PPAR expression it was hypothesised that a change in SIRT1expression correlates with the expression of either PPAR α /γ during DOX induced toxicity. We here investigated that whether SIRT-1 can modulate the homeostasis through transcriptional regulation of the PPARs in *Gg* treated as well as DOX treated H9c2 cardiomyocytes. In this experiment, SIRT-1 RNAi was employed which efficiently knocked down the SIRT-1 expression in H9c2 cells. By Western blot we analysed that upon SIRT-1 downregulation, the endogenous PPAR-α & γ expression was found to be reduced in SIRT-1 knockdown DOX treated H9c2 cardiomyocytes (**Fig. 11A-D**). It is indicated that SIRT-1 mediated homeostasis in untreated and DOX treated H9c2 cardiomyocytes might be transcriptionally regulated by SIRT-1, however to ascertain the biological significance further studies are required.

Discussion

The success of DOX as chemotherapeutic anti-cancerous drug is well known. However, the side effects reported on cardiac functioning is the biggest hindrance to its utility. Cardiomyopathy and congestive heart failure associated with DOX has remained a subject of debate from many years. To ameliorate the toxic effects of DOX while maintaining its efficacy against cancer, can be done by modifications in the chemical structure of the drug. Another approach is to add some supplements that maintain the anti-cancerous effect of DOX at the same time protect the normal tissue. In the present study, we demonstrated that the aqueous extract of the *G. glabra* (*Gg*) root has a potential against DOX-induced cardiotoxicity. We assessed morphological, metabolic, and molecular parameters to enumerate the success of phytoextract in DOX-elicited malformations in the cardiac myocytes where we found that 5 µM concentration of DOX was toxic to the H9c2 cardiomyocytes. Co-treatment with various concentrations of *Gg* on DOX-exposed cardiomyocytes proved effective as the cells displayed a recovery from cardiotoxicity. The anti-cancerous property *Gg* is well documented in different cancer cell lines viz. MCF-7 and HT-29 colon cells (Rathi *et al.,* 2009; Jo *et al.,* 2005; Nazmi, *et al.,* 2018 & Nourazarian *et al.,* 2016). To rule out any interference of the phytoextract with the anti-cancerous property of DOX, we simultaneously designed an experimental study with breast cancer line (MDA-MB). The aqueous extract of *Gg* with DOX inhibited the proliferation up to 60 % in MDA-MB similar to DOX alone as compared to control untreated H9c2 cardiomyocytes.

DOX treatment caused degradation of F-Actin and alteration in cardiac cell morphology while treatment with *Gg* countered the stress restoring F-actin to normal state. Similar effects of DOX on F-actin were reported in other cell lines (Guven *et al.,* 2016). A disrupted membrane can cause the leakage of LDH from damaged cells which were observed in present study. While in the presence of *Gg,* DOX-treated cells exhibited lesser LDH content, clearly indicating that the extracts were helpful in keeping the membrane intact and cell integrity (Sun *et al.,* 2013).

According to the previous report, aqueous *Gg* extract contains vital phytochemicals with antioxidant property to reduce the ROS generation (Visavadiya *et al.,* 2009). This free radical scavenging activity of *Gg* might be helping the cardiomyocytes from a redox imbalance produced under the influence of DOX. NBT and two redox sensitive fluorescent probes, DHE and H_2DCFDA, interact with free radicals [superoxide ($O_2^{-\cdot}$), hydroxyl, peroxyl-generated molecules]. Our study suggests that *Gg* exhibits potential antioxidant activity to counter the DOX-mediated oxidative stress in H9c2 cells.

Mitochondria is the primary source of free radical generation intervening during the pathological conditions. Numerous studies have supported that DOX-triggered free radicals can promote cumulative changes in mitochondrial structure and bioenergetics function which is considered as an early indicator of DOX-induced apoptosis or necrosis (Green and Leeuwenburgh, 2002). Mitochondrial ROS and membrane potential were determined to elucidate the ill effects of DOX on H9c2 cardiomyocytes. MitoSOX assay established that the level of mitochondrial ROS increases upon treatment with DOX similar to a report by Mukopadhyay and group. We analysed that the plant *Gg* aqueous extract significantly inhibited the DOX-induced H9c2 apoptosis, including $\Delta\Psi m$ dissipation and mitochondrial ROS (Mukhopadhyay *et al.,* 2007 & Lebrecht, *et al.,* 2003).

The free radical carriers have been recognized to vitiate the function of various cellular components such as those present at molecular as well as biochemical level. DOX-induced DNA damage was detected with 8-oxo-dG (Ferreira *et al.,* 2007 & Van Berlo *et al.,* 2010). DOX can react with nitrogen bases (purines and pyrimidines), a marker of ROS-generated genotoxicity hence damaging the DNA. Our results showed that introduction of aqueous extract before DOX, shielded the cardiomyocytes *in vitro* against the oxidative damage to DNA induced by DOX. Further it can be attributed that DOX-induced oxidative stress increases the cardiac nitric oxide (NO) that is associated with a corresponding rise in the iNOS gene expression (Mungrue *et al.,* 2002). We reported a similar result with iNOS in the presence of DOX; however, *Gg* extracts enhanced the iNOS expression. On the other hand, a marked decrease in the expression of SOD1 and SOD2 in DOX-treated H9c2 cells as

compared to the control cells suggests for an oxidative environment in cardiomyocytes whereas; *Gg* restored the SOD expression to ameliorate the stress conditions.

DOX is responsible for metabolic disturbance at different levels; Oil Red O marks the lipid accumulation, an indicator of disturbance in lipid homeostasis and a pathological condition of cardiomyopathy. We here investigated that DOX treatment accumulated the lipid in the cells whereas the *Gg* extract when given before the DOX retain the non-pathological condition by diminishing the lipid accumulation in H9c2 cardiomyocytes. A possible reason of lipid accumulation could be downregulation of PPAR-γ, which disturbs lipid transportation and the condition resulting to its accumulation (Arunachalam *et al.*, 2013).

SIRT-1 which is a nuclear localized NAD^+-dependent deacetylase factor, maintains the metabolic homeostasis contributing in various biological processes including cell cycle, apoptosis, gene silencing, and energy homeostasis and PPARs, also regulate lipid metabolism and energy balance (Rahmatollahi *et al.*, 2016). We extensively analysed the protein and gene expression of these functional proteins. H9c2 cells showed a drastic down-regulation in SIRT-1 expression on exposure to DOX while, *Gg* improved its expression in the presence of DOX. We hypothesize that the imperative role of *Gg* extract might involve both SIRT-1 and PPAR-α & γ, which can be defensive against DOX-induced cardiotoxicity. Further we also found that the expression levels of both SIRT-1 and PPAR-γ reduced in the total cell lysates while, that of PPAR-α elevated in DOX-treated cells which is in accordance with previous reports (Liu *et al.*, 2016). While PPAR-γ has been reported to improve the cardiac health from pathological conditions as widely mentioned (Rahmatollahi *et al.*, 2016) on the other hand, the expression of PPAR-α has till date remained uncertain.

To further gather information about compartmentalization of SIRT-1 and PPARs proteins within the cell, we evaluated their expression in cytoplasm as well as nuclei. We observed that the SIRT-1 and PPAR-γ do not translocate to the nuclei from cytoplasm during the DOX-treatment. Treatment with *Gg* alongwith DOX neutralizes the effect of DOX alone and helped in restoring their normal expression in nuclei implying that SIRT-1 and PPAR-γ have some protective role to play against DOX-mediated cardiotoxicity. The PPAR-α levels were decreased in nuclei when treated with DOX however *Gg* alongwith DOX increased its expression in nuclei. It is reported that PPAR-α regulates SIRT-1 through feedback inhibition as the level of former increases. It is not clear how DOX affects the cytoplasmic nuclear shuttling of PPAR and SIRT-1, one possible explanation is via affecting the intracellular Ca^{2+} regulation, which play a significant role in nucleo-cytoplasmic shuttling of PPARs as explained by Umemoto and Fujiki.

It is further verified that PPAR-α, in the free form, translocates to the nucleus and is responsible for activation of transcription factors associated with hypertrophy and apoptosis. To confirm whether SIRT-1 transcription affects the synthesis of PPAR-α and -γ, the mRNA levels of SIRT-1 and PPARs was evaluated. It was observed that mRNA levels of SIRT-1 and PPAR-α was significantly decreased in DOX treated H9c2 cells whereas no significant change was observed in PPAR-γ gene expression. *Gg* treatment protected the cardiomyocytes against DOX through influencing the expression of SIRT-1 and PPAR-α & γ mediated pathways.

Hypertrophy is the penultimate step of cardiomyocyte death; various hypertrophic markers are up-regulated during arterial hypertension in ventricular myocytes and cardiomyocytes that gradually proceed to apoptosis. ANP and BNP are the members of natriuretic peptide (NP) family that are highly correlated to the hypertrophic ventricles and are considered for clinical diagnostic and prognostic implications (De Bold *et al.*, 2011). Upon introduction of DOX, the expression of these genes increased in H9c2 cardiomyocytes presenting a similar hypertrophic condition. Supplementation with *Gg*, reduced cardiomyocytes damage as well as expression of ANP and BNPs. On the contrary, the level of other cardiac development marker, GATA increased in the presence DOX, while *Gg* extracts also had similar effects on their expression. A clear conclusion cannot be drawn, although an increased expression of GATA6 upon treatment of *Gg* depicts its role in preventing the catastrophic effects of DOX.

The effect of DOX on muscle contraction which is an important physiological cardiac phenomenon was also evaluated. We examined the protein expression of some contractile proteins MLC2v, MHC, troponin I. DOX markedly increased the level of MHC and troponin-I expression. The expression of *MLC2v* gene increased whereas its protein level was found to be decreased with the DOX treatment.

Based on the above analysis, it is further hypothesized that there is an interaction between PPAR and SIRT-1 next we performed co-immunoprecipitation based experiments. It was observed that PPAR-α has displayed interaction in normal condition, while DOX reduced this interaction. While in *Gg* co-treated cells, a negative inhibition of SIRT-1 through PPAR-α was observed. The physical interactions between SIRT1 and PPAR proteins have been investigated suggesting that the PPAR α is an influential component in SIRT-1 mediated signalling. In H9c2 cardiomyocytes, SIRT-1 showed an interaction in control and *Gg*-treated H9c2 cardiomyocytes with PPAR-α. SIRT-1 de-acetylate the PPAR-α in cardiomyocytes which further activates the PPAR-α. It is also supported that PPAR-α mediates in various physiological processes which are regulated by SIRT-1 signalling (Purushotham *et al.*, 2009).

To further verify the hypothesis, that SIRT-1 influences the expression of PPAR-α & γ, we employed SIRT-1 RNAi technique to specifically knock down this pathway. siRNA mediated knockdown of SIRT-1 in reduced the endogenous PPAR-α & γ expression in DOX treated H9c2 cardiomyocytes suggesting SIRT-1 mediated homeostasis during DOX-induced treated cardiac toxicity, however to ascertain the biological significance additional studies will be conducted in near future.

Conclusion

Our *in vitro* studies dealt with toxic effects of DOX on H9c2 cardiomyocytes mediated through influencing the cellular homeostasis and lipid metabolism. These two processes are regulated by SIRT-1 and PPARs. Besides this, DOX induced ROS was also responsible for DNA base damage and influenced the expression of various proteins at transcriptional and translational level. The antioxidant properties of *Gg* root extract reconcile the cellular homeostasis by scavenging the ROS level and their adverse consequences via modulating the SIRT-1 and PPARs. Further studies need to be conducted which will shed light on the mechanism to improve the therapeutic effects of chemotherapeutic drugs in order to minimise the normal tissue damage without changing the anti-cancer efficacy.

Acknowledgement

Funding Agency: S.U. acknowledges the financial support in the form of SRF from ICMR, New Delhi. This work has been supported by the DST Young Investigator Fast Track Grant (SB/4S/LS107/2013) to Dr. Monisha Dhiman.

We thank Mr. Ashish K. Pandey and Dr. Sumeer Razdaan (Central Instrumentation Laboratory, CUPB) for their help with the imaging and other technical expertise.

Conflict of interest: The authors declare that they have no conflict of interest.

Ethical Approval: None

References

Al-Obaidi, O. H. S. (2013). Aqueous and Alcohol Extraction of Plant (*Glycyrrhiza glabra)* and activity study against bacteria and Cancer (Cell Line RD). European Chemical Bulletin, 3(2), 133-137.

Ammar, N. M., El-Hawary, S. S. E. D., El-Anssary, A. A., Othman, N., Galal, M., & El-Desoky, A. H. (2012). Phytochemical and clinical studies of the bioactive extract of *Glycyrrhiza glabra L*. Family Leguminosae. International Journal of Phytomedicine, 4(3), 429.

Arunachalam, S., Pichiah, P. T., & Achiraman, S. (2013). Doxorubicin treatment inhibits PPARγ and may induce lipotoxicity by mimicking a type 2 diabetes-like condition in rodent models. FEBS Letters, 587(2), 105-110.

Barger, P. M., Brandt, J. M., Leone, T. C., Weinheimer, C. J., & Kelly, D. P. (2000). Deactivation of peroxisome proliferator–activated receptor-α during cardiac hypertrophic growth. Journal of Clinical Investigation, 105(12), 1723-1730.

De Bold, A. J., Ma, K. K. Y., Zhang, Y., de Bold, M. L. K., Bensimon, M., & Khoshbaten, A. (2001). The physiological and pathophysiological modulation of the endocrine function of the heart. Canadian Journal of Physiology and Pharmacology, 79(8), 705-714.

Dhiman, M., & Garg, N. J. (2011). NADPH oxidase inhibition ameliorates *Trypanosoma cruzi*-induced myocarditis during Chagas disease. The Journal of Pathology, 225(4), 583-596.

Dhiman, M., Wan, X., Popov, V. L., Vargas, G., & Garg, N. J. (2013). Mn SOD tg Mice Control Myocardial Inflammatory and Oxidative Stress and Remodeling Responses Elicited in Chronic Chagas Disease. Journal of the American Heart Association, 2(5), e000302.

Dhingra D, Parle M, Kulkarni SK (2004) Memory enhancing activity of *Glycyrrhiza glabra* in mice. J Ethnopharmacol 91(2–3), 361–365.

Dolinsky, V. W. (2017). The role of sirtuins in mitochondrial function and doxorubicin-induced cardiac dysfunction. Biological Chemistry, 398(9), 955-974.

Ferreira, A.L.A., Salvadori, D. M. F., Nascimento, M. C., Rocha, N. S., Correa, C. R., Pereira, E. J., Ladeira, M. S. P., et al., (2007). Tomato-oleoresin supplement prevents doxorubicin-induced cardiac myocyte oxidative DNA damage in rats. Mutation Research/Genetic Toxicology and Environmental Mutagenesis, 631(1), 26-35.

Franceschelli, S., Pesce, M., Ferrone, A., Patruno, A., Pasqualone, L., Carlucci, G., Felaco, M. et al. (2016). A novel biological role of α-mangostin in modulating inflammatory response through the activation of SIRT-1 signaling pathway. Journal of Cellular Physiology, 231(11), 2439-2451.

Green, P. S., & Leeuwenburgh, C. (2002). Mitochondrial dysfunction is an early indicator of doxorubicin-induced apoptosis. Biochimica et Biophysica Acta (BBA)-Molecular Basis of Disease, 1588(1), 94-101.

Gupta, K. B., Upadhyay, S., Saini, R. G., Mantha, A. K., & Dhiman, M. (2018). Inflammatory response of gliadin protein isolated from various wheat varieties on human intestinal cell line. Journal of Cereal Science, 81, 91-98.

Gupta, S., Bhatia, V., Wen, J. J., Wu, Y., Huang, M. H., & Garg, N. J. (2009). *Trypanosoma cruzi* infection disturbs mitochondrial membrane potential and ROS production rate in cardiomyocytes. Free Radical Biology and Medicine, 47(10), 1414-1421.

Guven, C., Taskin, E., & Akcakaya, H. (2016). Melatonin prevents mitochondrial damage induced by doxorubicin in mouse fibroblasts through AMPK-PPAR gamma-dependent mechanisms. International Medical Journal of Experimental and Clinical Research, 22, 438.

Han, L., Zhou, R., Niu, J., McNutt, M. A., Wang, P., & Tong, T. (2010). SIRT1 is regulated by a PPARγ–SIRT1 negative feedback loop associated with senescence. Nucleic Acids Research, 38(21), 7458-7471.

Hrelia, S., Fiorentini, D., Maraldi, T., Angeloni, C., Bordoni, A., Biagi, P. L., & Hakim, G. (2002). Doxorubicin induces early lipid peroxidation associated with changes in glucose transport in cultured cardiomyocytes. Biochimica et Biophysica Acta (BBA)-Biomembranes, 1567, 150-156.

Hsu, C. P., Zhai, P., Yamamoto, T., Maejima, Y., Matsushima, S., Hariharan, N., Sadoshima, J., et al. (2010). Silent information regulator 1 protects the heart from ischemia/reperfusion. Circulation, 122(21), 2170-2182.

Jo, E. H., Kim, S. H., Ra, J. C., Kim, S. R., Cho, S. D., Jung, J. W., Kim, T. Y. (2005). Chemopreventive properties of the ethanol extract of chinese licorice (*Glycyrrhiza uralensis)* root: induction of apoptosis and G1 cell cycle arrest in MCF-7 human breast cancer cells. Cancer Letters, 230(2), 239-247.

Lebrecht, D., Setzer, B., Ketelsen, U. P., Haberstroh, J., & Walker, U. A. (2003). Time-dependent and tissue-specific accumulation of mtDNA and respiratory chain defects in chronic doxorubicin cardiomyopathy. Circulation, 108(19), 2423-2429.

Levrand, S., Pesse, B., Feihl, F., Waeber, B., Pacher, P., Rolli, J., Liaudet, L., et al.(2005). Peroxynitrite is a potent inhibitor of NF-κB activation triggered by inflammatory stimuli in cardiac and endothelial cell lines. Journal of Biological Chemistry, 280(41), 34878-34887

Liu, M. H., Shan, J., Li, J., Zhang, Y., & Lin, X. L. (2016). Resveratrol inhibits doxorubicin induced cardiotoxicity via sirtuin 1 activation in H9c2 cardiomyocytes. Experimental and Therapeutic Medicine, 12(2), 1113-1118.

Ma, D., Wei, H., Lu, J., Ho, S., Zhang, G., Sun, X., & Wong, P., et al. (2012). Generation of patient-specific induced pluripotent stem cell-derived cardiomyocytes as a cellular model of arrhythmogenic right ventricular cardiomyopathy. European Heart Journal, 34(15), 1122-1133.

Montaigne, D., Hurt, C., & Neviere, R. (2012). Mitochondria death/survival signaling pathways in cardiotoxicity induced by anthracyclines and anticancer-targeted therapies. Biochemistry Research International, 2012, 951539.

Mukhopadhyay, P., Rajesh, M., Yoshihiro, K., Haskó, G., & Pacher, P. (2007). Simple quantitative detection of mitochondrial superoxide production in live cells. Biochemical and Biophysical Research Communications, 358(1), 203-208.

Mungrue, I. N., Gros, R., You, X., Pirani, A., Azad, A., Csont, T., Husain, M., et. al. (2002). Cardiomyocyte overexpression of iNOS in mice results in peroxynitrite generation, heart block, and sudden death. Journal of Clinical Investigation, 109(6), 735-743.

Nazmi, S. A., Nourazarian, A., Bahhaj, R., & Khakikhatibi, F. (2018). The Anticancer Effect of *Arctium lappa* and *Glycyrrhiza glabra* on HT-29 Colon Cancer and MCF-7 Breast Cancer Cell Lines. Cancer, 6, 7.

Nourazarian, S. M., Nourazarian, A., Majidinia, M., & Roshaniasl, E. (2016). Effect of root extracts of medicinal herb Glycyrrhiza glabra on HSP90 gene expression and apoptosis in the HT-29 colon cancer cell line. Asian Pacific Journal of Cancer Prevention, 16(18), 8563-8566.

Oka, S. I., Zhai, P., Alcendor, R., Park, J. Y., Tian, B., & Sadoshima, J. (2012). Suppression of ERR targets by a PPARα/Sirt1 complex in the failing heart. Cell Cycle, 11(5), 856-864.

Planavila, A., Rodríguez-Calvo, R., Jové, M., Michalik, L., Wahli, W., Laguna, J. C., & Vázquez-Carrera, M. (2005). Peroxisome proliferator-activated receptor β/δ activation inhibits hypertrophy in neonatal rat cardiomyocytes. Cardiovascular Research, 65(4), 832-841.

Purushotham, A., Schug, T. T., Xu, Q., Surapureddi, S., Guo, X., & Li, X. (2009). Hepatocyte-specific deletion of SIRT1 alters fatty acid metabolism and results in hepatic steatosis and inflammation. Cell Metabolism, 9(4), 327-338.

Rahmatollahi, M., Baram, S. M., Rahimian, R., Saravi, S. S. S., & Dehpour, A. R. (2016). Peroxisome Proliferator-Activated Receptor-α Inhibition Protects Against Doxorubicin-Induced Cardiotoxicity in Mice. Cardiovascular Toxicology, 16(3), 244-250.

Rathi, S. G., Suthar, M., Patel, P., Bhaskar, V. H., & Rajgor, N. B. (2009). In-vitro cytotoxic screening of *Glycyrrhiza glabra L.* (Fabaceae): A natural anticancer drug. Journal of Young Pharmacists, 1(3), 239.

Sarkar B, Kulharia M, Mantha AK (2017). Understanding human thiol dioxygenase enzymes: structure to function, and biology to pathology. International Journal of Experimental Pathology, 98 (2), 52-66.

Sarkar, B., Dhiman, M., Mittal, S., & Mantha, A. K. (2017). Curcumin revitalizes Amyloid beta (25–35)-induced and organophosphate pesticides pestered neurotoxicity in SH-SY5Y and IMR-32 cells via activation of APE1 and Nrf2. Metabolic Brain Disease, 32(6), 2045-2061.

Strigun, A., Wahrheit, J., Niklas, J., Heinzle, E., & Noor, F. (2011). Doxorubicin increases oxidative metabolism in HL-1 cardiomyocytes as shown by 13C metabolic flux analysis. Toxicological Sciences, 125(2), 595-606.

Sun, J., Sun, G., Meng, X., Wang, H., Luo, Y., Qin, M., Sun, X., et al. (2013). Isorhamnetin protects against doxorubicin-induced cardiotoxicity *in vivo* and *in vitro*. PloS One, 8(5), e64526.

Umemoto, T., & Fujiki, Y. (2012). Ligand dependent nucleo-cytoplasmic shuttling of peroxisome proliferatoractivated receptors, PPARα and PPARγ. Genes to Cells, 17(7), 576-596.

Upadhyay, S., Vaish, S., & Dhiman, M. (2019). Hydrogen peroxide-induced oxidative stress and its impact on innate immune responses in lung carcinoma A549 cells. Molecular and Cellular Biochemistry, 450(1-2), 135-147.

Van Berlo, J. H., Elrod, J. W., Van Den Hoogenhof, M. M., York, A. J., Aronow, B. J., Duncan, S. A., et al. (2010). The transcription factor GATA-6 regulates pathological cardiac hypertrophy. Circulation Research, 107(8), 1032-1040.

Visavadiya, N. P., Soni, B., & Dalwadi, N. (2009). Evaluation of antioxidant and anti-atherogenic properties of *Glycyrrhiza glabra* root using *in vitro* models. International Journal of Food Sciences and Nutrition, 60(supp2), 135-149.

List of Abbreviations

DOX: Doxorubicin

Gg: *Glycyrrhiza glabra*

MLC-2: Myosin Light Chain 2

NOS: Nitric Oxide Synthase

PPAR: Peroxisomes Proliferator-Activated Receptors

RNS: Reactive Nitrogen Species

ROS: Reactive Oxygen Species

Figure Legends

Fig.1. A) Effect of DOX alone on percentage of viability against DOX-induced cytotoxicity in H9c2 cardiomyocytes. **B)** The cardiomyocytes were pre-treated with different concentrations (20-200 µg/ml) of *Gg* along with 5µM of DOX for 24 hr. **C)** The selected concentration (40µg/ml) of *Gg* along with DOX was used in MDA-MB cancer cell line. Data is represented as Mean + SD from three separate experiments. The untreated control is considered as 100, where * indicates the significance level when the DOX treated cells are compared with untreated control (***P≤0.001, **P≤0.005) and $ indicates the significance level when the DOX + *Gg* treated cells are compared with DOX alone ($P≤0.01).

Fig. 2. Representative microscopic images of H9c2 cardiomyocytes when treated with DOX alone (5 µM) and DOX + *Gg* (40µg/ml). **A)** H9c2 cardiomyocytes stained with haematoxylin to visualise the cell structure and morphology. **B)** Confocal microscopic images showing Hoescht 33342 staining for nuclei (Panel-1), phalloidin staining for F-actin (Panel-2) and merged image (Panel-3). Images indicates the disintegration of Actin in the presence of DOX alone while *Gg* protects F-Actin disintegration. **C)** The membrane integrity of H9c2 cells was detected using LDH assay. Data is represented as Mean + SD from three separate experiments. The untreated control is considered as 100, where * indicates the significance level when the DOX treated cells compared with untreated control (***P≤0.001) and $ indicates the significance level when the DOX + *Gg* treated cells are compared with DOX alone ($P≤0.01).

Fig. 3. The figure represent level of reactive oxygen species (ROS) generated in H9c2 cells when exposed to selected concentration of DOX and DOX+*Gg*, ROS was detected using **A)** NBT assay. **B)** H_2DCFDA based assay and **C)** DHE assay. Data is expressed as Mean± SD, untreated control is considered as 100, where *indicates the significance level when the DOX treated cells are compared with untreated control (***P≤0.001, **P≤0.005) and $ indicates the significance level when the DOX + *Gg* treated cells are compared with DOX alone ($P≤0.01).

Fig. 4. Figure showing the mitochondrial ROS and mitochondrial membrane potential in H9c2 cardiomyocytes when treated with selected concentration of DOX and DOX+*Gg*. The confocal images showing: **A- Panel 1)** DAPI stained cells; **Panel 2)** Mitochondrial ROS detected stained with MitoSOX and **Panel 3)** Quality of mitochondria stained with mitotracker. The scale bar for the confocal imaging is 10µM. **B)** The mitochondrial membrane potential was detected using JC-1 probe. For JC-1 staining the data is represented

as Mean±SD, untreated control is considered as 100, where *indicates the significance level when the DOX treated cells are compared with untreated control (***P $\leq$0.001) and $ indicates the significance level when the DOX + *Gg* treated cells are compared with DOX alone ($^{\$}P\leq$0.01).

Fig.5. Oxidative stress induced DNA damage in DOX and DOX+*Gg* treated H9c2 cardiomyocytes was detected. Representative confocal images to detect the oxidative stress induced DNA damage using 8-Oxo-dG and Alexa Flour-488 as primary and secondary antibodies respectively.

Fig.6. Western blotting was performed in the DOX and DOX+*Gg* treated cell lysate to detect the level of oxidant and antioxidant enzymes; **A)** NOS2; SOD1 and SOD2. Densitometry was performed to quantify the protein expression of; **B)** NOS1; **C)** SOD1; and **D)** SOD2. The data is represented as Mean±SD, where *indicates the significance level when the DOX treated cells are compared with untreated control (**P $\leq$0.005) and $ indicates the significance level when the DOX + *Gg* treated cells are compared with DOX alone ($^{\$}P\leq$0.01).

Fig.7. The lipid homoeostasis in the DOX and DOX+*Gg* treated cardiomyocytes was detected using **A)** Oil red O staining. In the in the DOX and DOX+*Gg* treated cardiomyocytes the levels of cardiac metabolic markers SIRT-1, PPAR-γ and PPAR-α, was detected by; **B)** Western Blot analysis **C)** Relative expression of protein was quantified with densitometry where data is represented as Mean±SD, where *indicates the significance level when the DOX treated cells are compared with untreated control (**P $\leq$0.005 & *P $\leq$0.01) and $ indicates the significance level when the DOX + *Gg* treated cells are compared with DOX alone ($^{\$}P\leq$0.01). **D)** q-PCR was performed to analyse the mRNA levels of cardiac metabolic markers SIRT-1, PPAR-γ and PPAR-α.

Fig. 8. A) Western blot was performed to detect the protein expression of SIRT-1, PPAR-γ, PPAR-α in cytoplasmic extracts of the cells treated with selected concentration of DOX and DOX+*Gg*. **B)** Densitometric analysis of SIRT-1; **C)** PPAR-γ and **D)** PPAR-α. **E)** Western blot was also performed to detect the protein expression of SIRT-1, PPAR-γ, PPARα in nuclear lysates of the cells treated with selected concentration of DOX and DOX+*Gg*. **F)** Densitometric analysis of SIRT-1; **G)** Densitometric analysis of PPAR-γ and **H)** Densitometric analysis of PPAR-α in nuclear lysates. Data represented as Mean±SD, where *indicates the significance level when the DOX treated cells are compared with untreated control (**P $\leq$0.005 & *P $\leq$0.01) and $ indicates the significance level when the DOX + *Gg* treated cells are compared with DOX alone ($^{\$}P\leq$0.01).

Fig. 9. The protein and mRNA expression of various hypertrophy markers was detected in cells treated with selected concentration of DOX and DOX+*Gg*. **A)** Western blot analysis of protein expression of MLC, MHC and troponin-I. **B)** Densitometric analysis of MLC; **C)** Densitometric analysis of MHC and **D)** Densitometric analysis of troponin-I. Data represented as Mean±SD, where *indicates the significance level when the DOX treated cells are compared with untreated control (**P $\leq$0.005 & *P $\leq$0.01) and $ indicates the significance level when the DOX + *Gg* treated cells are compared with DOX alone ($^{\$}P\leq$0.01). **E)** Real-Time PCR was also performed to observe the mRNA levels of hypertrophic markers MLC2v, ANP, BNP, GATA-4 and GATA-6.

Fig.10. Co-immunoprecipitation studies to evaluate the interaction of SIRT-1 with PPAR-γ, PPAR-α**. A)** Anti-PPAR-α antibody-immunoprecipitated proteins were analysed by Western blotting with anti-SIRT1 antibody in total cell lysates (TCL) and immunoprecipitated samples. **B)** Anti-PPAR-γ antibody-immunoprecipitated proteins were analysed by Western blotting with anti-SIRT1 antibody in total cell lysates (TCL) and immunoprecipitated samples. **C)** STRING analysis to elucidate the PPARs and SIRT-1 interaction. Probability of Interaction of SIRT-1 (score: 0.420 and 0.481) is not significant with either PPAR-α or PPAR-γ respectively.

Fig.11. To elucidate the role of SIRT-1 in regulating PPAR expression the H9c2 cardiomyocytes were transfected with si-SIRT-1 followed by treatment with DOX and DOX+*Gg*. **A)** Western blot was performed for the proteins expression of SIRT-1, PPAR-γ and PPARα, in the si-SIRT-1 tranfected cell lysate. The intensity of the protein bands was analysed with the densitometric analysis for the expression of; **B)** SIRT-1; **C)** PPAR-γ and **D)** PPAR-α in si-SIRT-1 tranfected H9c2 cardiomyocytes.

Table 1. Primers used for quantitative real-time PCR analysis

Gene name	Forward Primer (5'-3')	Reverse Primer (5'-3')
GAPDH	CTTCATTGACCTCAACTAC	GCCATCCACAGTCTTCTG
MLC-2v	CTCCAACGTGTTCTCCATG	AGTCCTTCTCTTCTCCGTGGG
PPAR-α	GTCCTCTGGTTGTCCCCTTG	TGGGGAGAGAGGACAGAT
PPAR-γ	GGGTACCGGGTCGTGTGA	AATAATAAGGCGGGGACGCA
SIRT-1	CCCAGATCCTCAAGCCATGTT	TGCTTTCCTTCCACTGCACA
GATA 4	GGGCCAGCAAAGTAAAAGGC	CTGGGAACAGCACCTAGTGG
GATA 6	GCCAACTGTCACACCACAAC	TTCATATAAAGCCCGCAAGC
BNP	CTTGGGCTGTGACGGGCTGAG	GCTGGGGAAAGAAGAGCCGCA
ANP	TGGGCTCCTTCTCCATCACC	GCCAAAAGGCCAGGAAGAGG

Table 2: Sequence of siRNA SIRT-1

siRNA SIRT-1	sense:5′-UUCUCCGAACGµGGCACGA -3' antisense:5′- UCU UUA UUC AUC AGG GAG GTT-3′
Control siRNA	sense: 5′-GAAGUµGACCUCCUCAUU-G3′, antisense:5′-CAA µGA GGA GGU CAA CUU-C3′

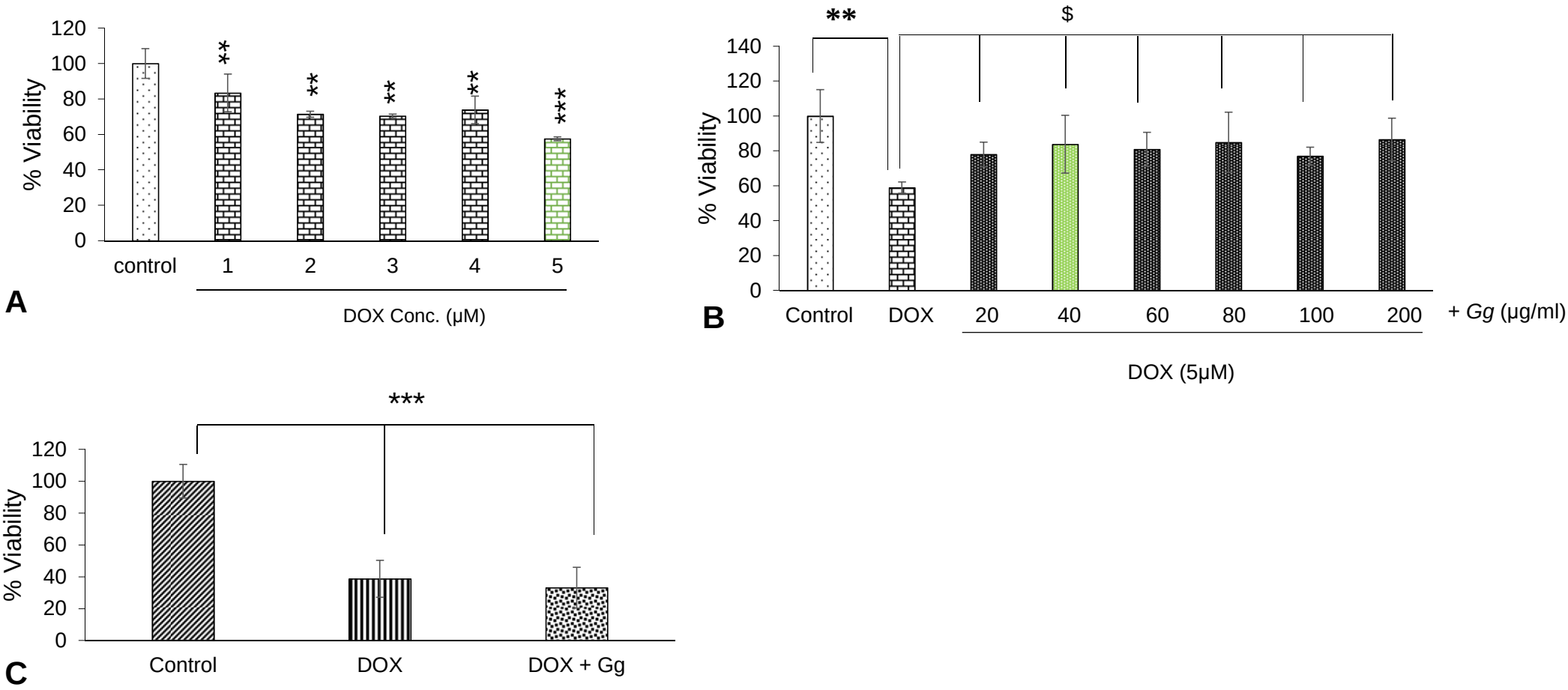
A
% Viability
120
100
80
60
40
20
0
**
**
**
**
***
control
1
2
3
4
5
DOX Conc. (μM)
B
**
$
% Viability
140
120
100
80
60
40
20
0
Control
DOX
20
40
60
80
100
200
+ Gg (μg/ml)
DOX (5μM)
C
***
% Viability
120
100
80
60
40
20
0
Control
DOX
DOX + Gg

Fig. 1.

Fig. 2.

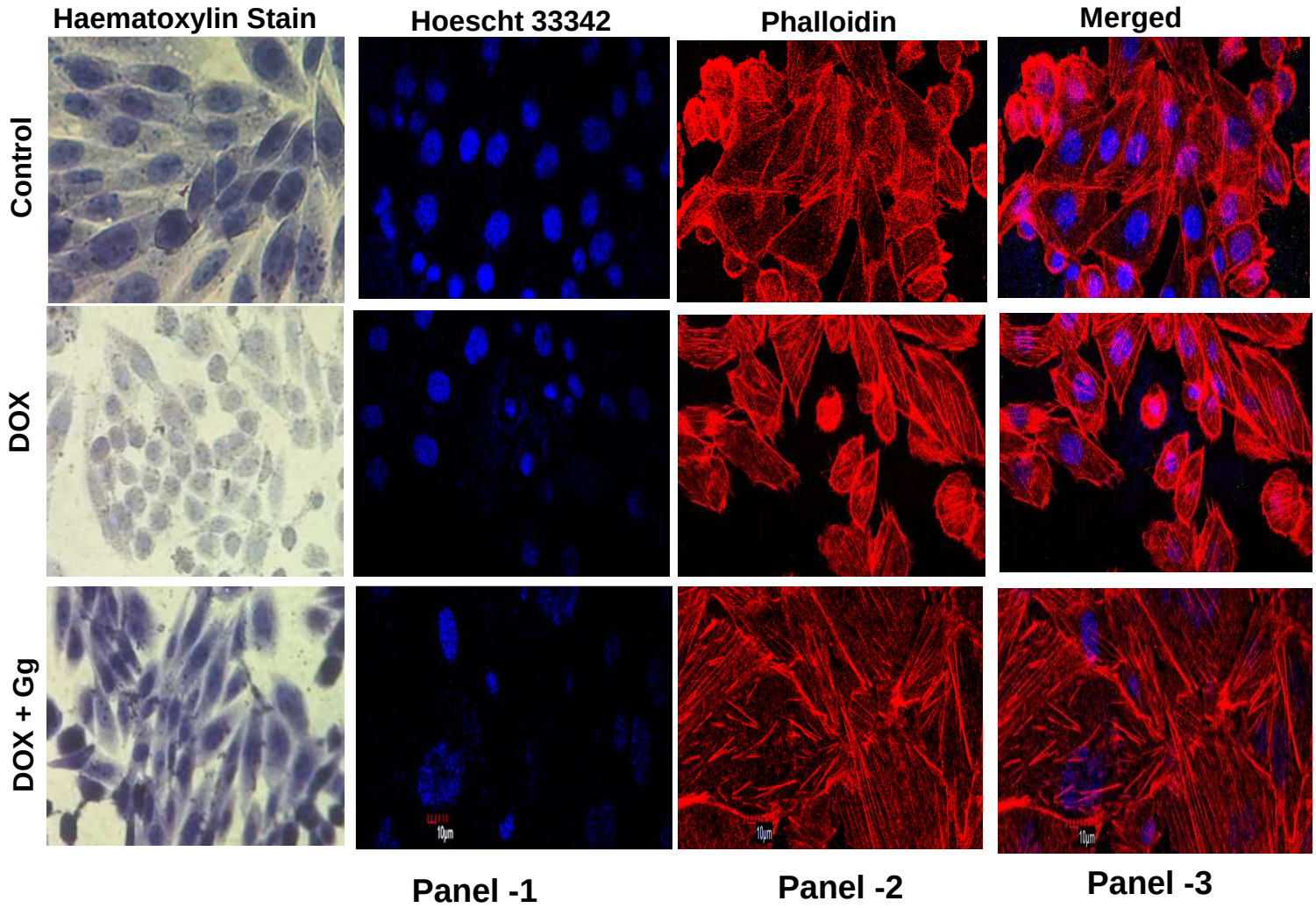
Haematoxylin Stain
Hoescht 33342
Phalloidin
Merged
Control
DOX
DOX + Gg
Panel -1
Panel -2
Panel -3
A
B

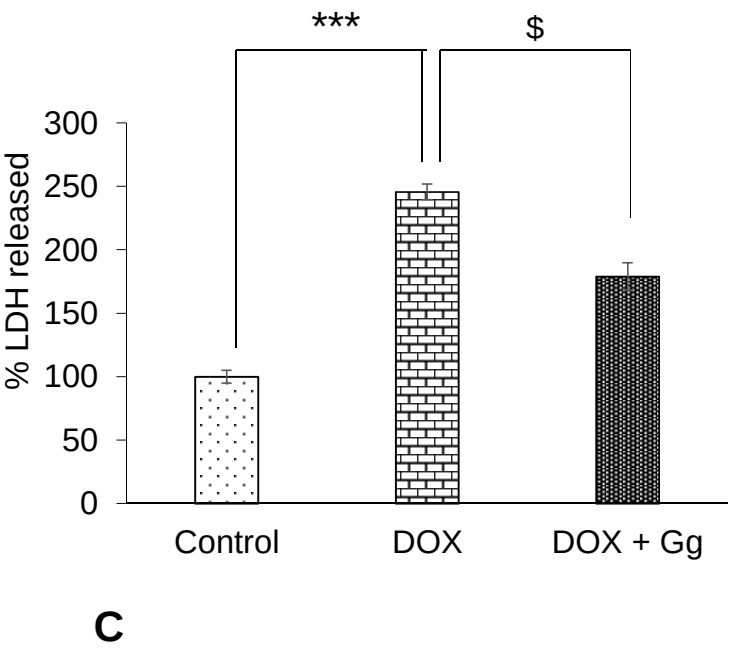
***
$
% LDH released
300
250
200
150
100
50
0
Control
DOX
DOX + Gg
C

Fig. 3.

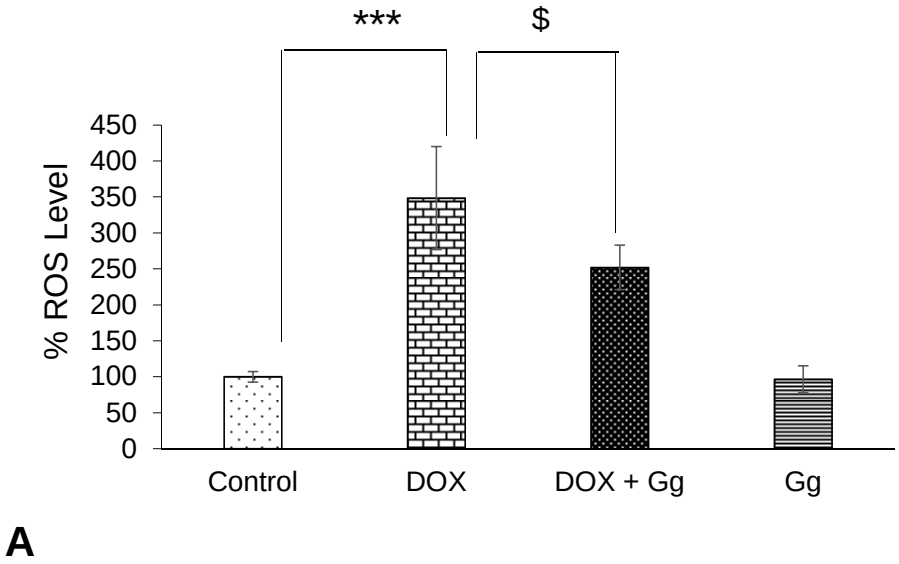
***
$
% ROS Level
450
400
350
300
250
200
150
100
50
0
Control
DOX
DOX + Gg
Gg

A

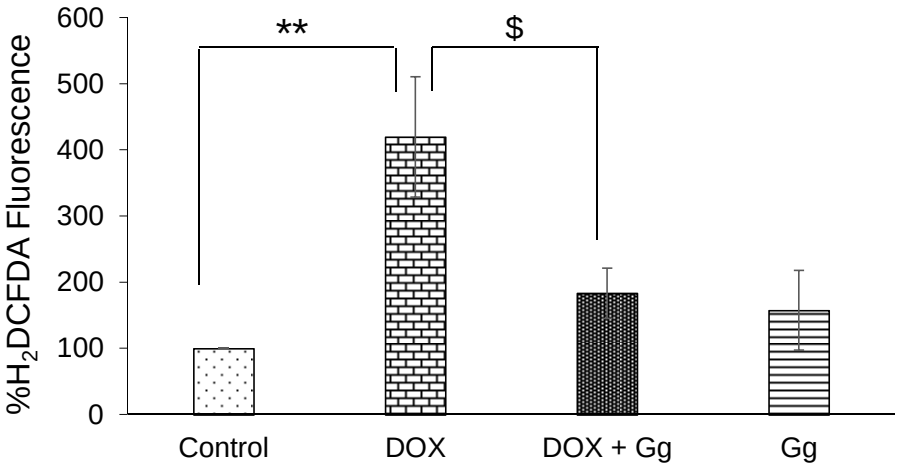
**
$
%H2DCFDA Fluorescence
600
500
400
300
200
100
0
Control
DOX
DOX + Gg
Gg

B

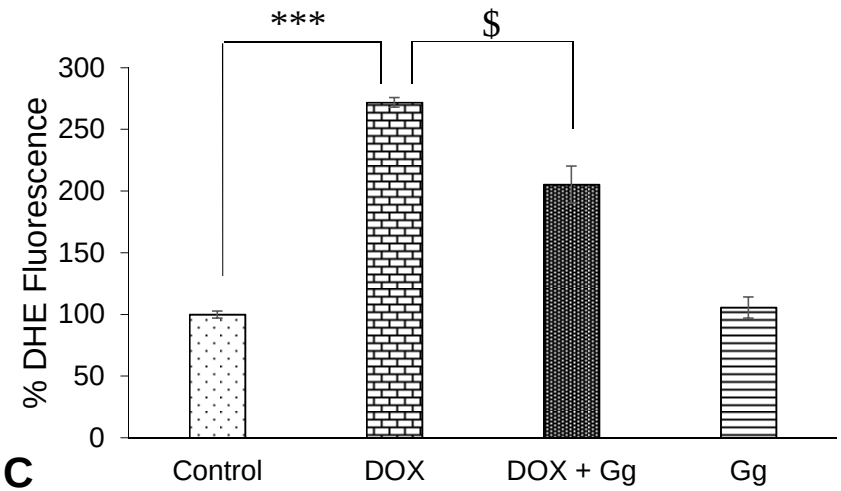
***
$
% DHE Fluorescence
300
250
200
150
100
50
0
Control
DOX
DOX + Gg
Gg

C

Fig. 4.

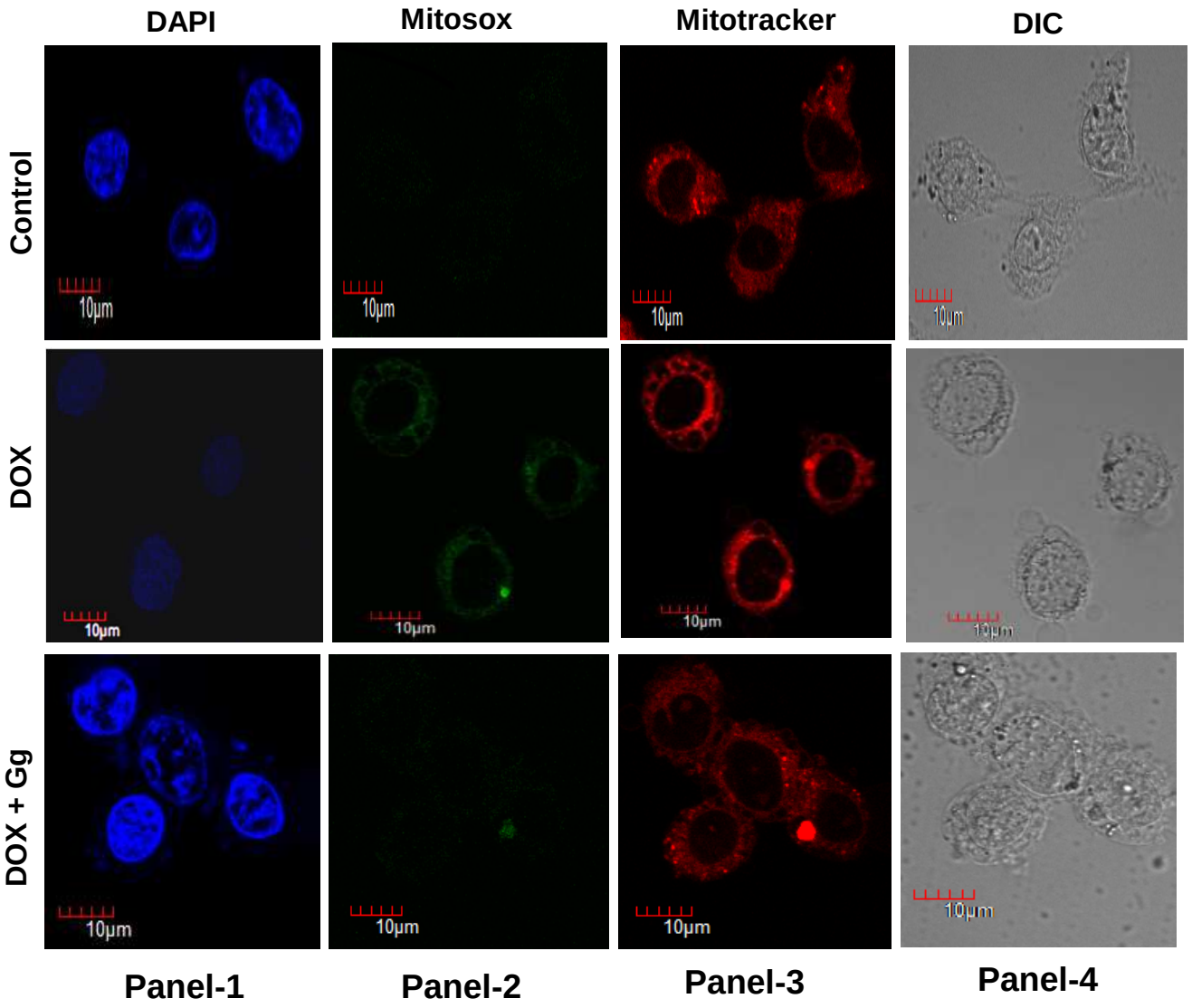
DAPI
Mitosox
Mitotracker
DIC
Control
DOX
DOX + Gg
10µm
Panel-1
Panel-2
Panel-3
Panel-4

A

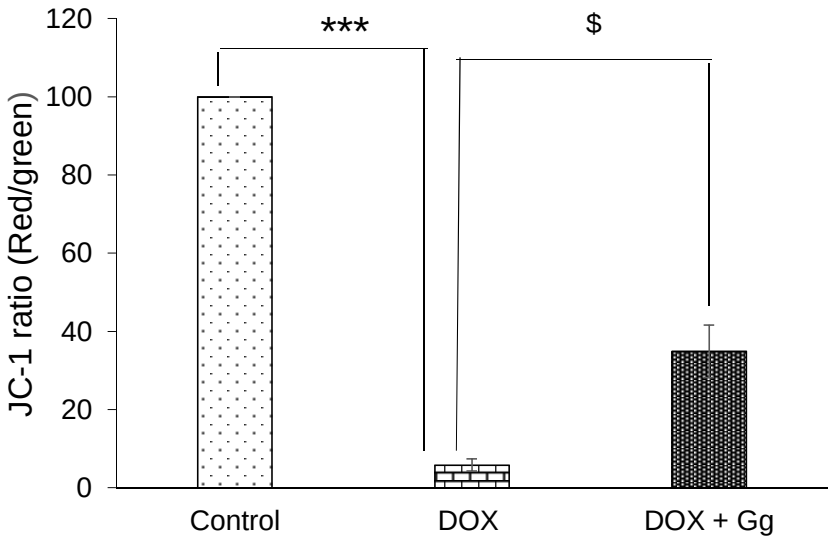
JC-1 ratio (Red/green)
120
100
80
60
40
20
0
***
$
Control
DOX
DOX + Gg

B

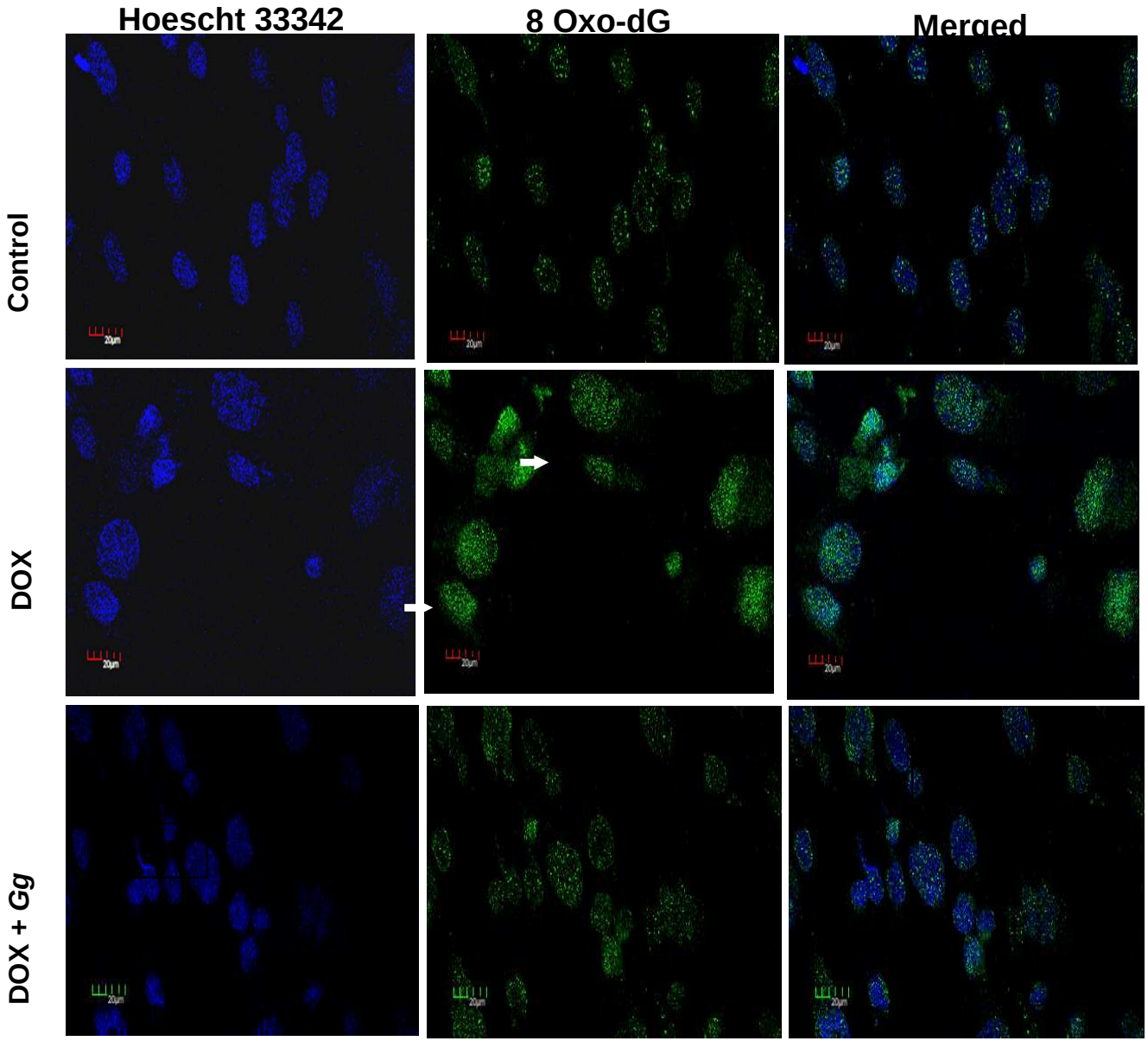

Fig. 5.

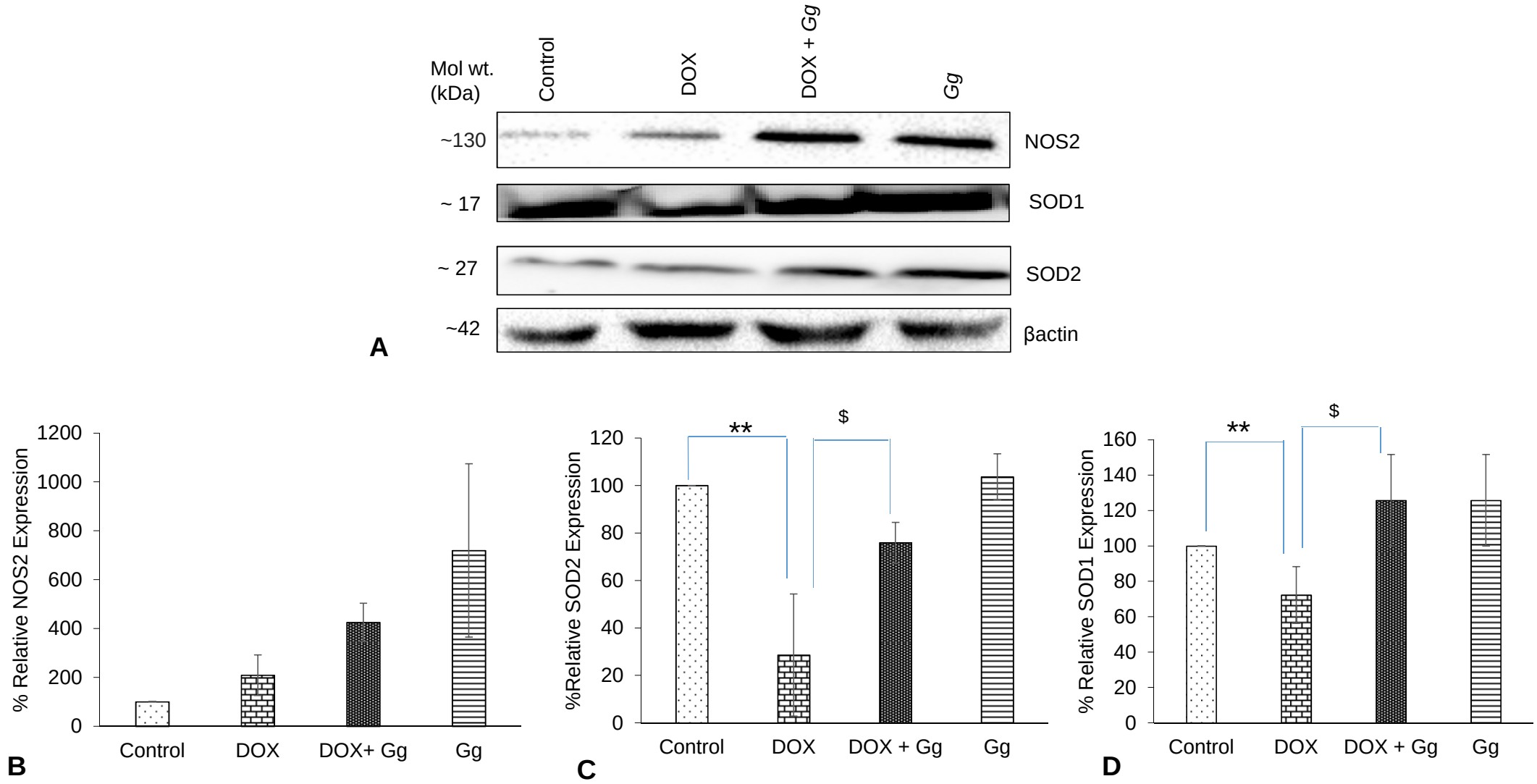
Mol wt. (kDa)
Control
DOX
DOX + Gg
Gg
~130
NOS2
~ 17
SOD1
~ 27
SOD2
~42
βactin
A
% Relative NOS2 Expression
1200
1000
800
600
400
200
0
Control
DOX
DOX+ Gg
Gg
B
%Relative SOD2 Expression
120
100
80
60
40
20
0
**
$
Control
DOX
DOX + Gg
Gg
C
% Relative SOD1 Expression
160
140
120
100
80
60
40
20
0
**
$
Control
DOX
DOX + Gg
Gg
D

Fig. 6.

Fig. 7.

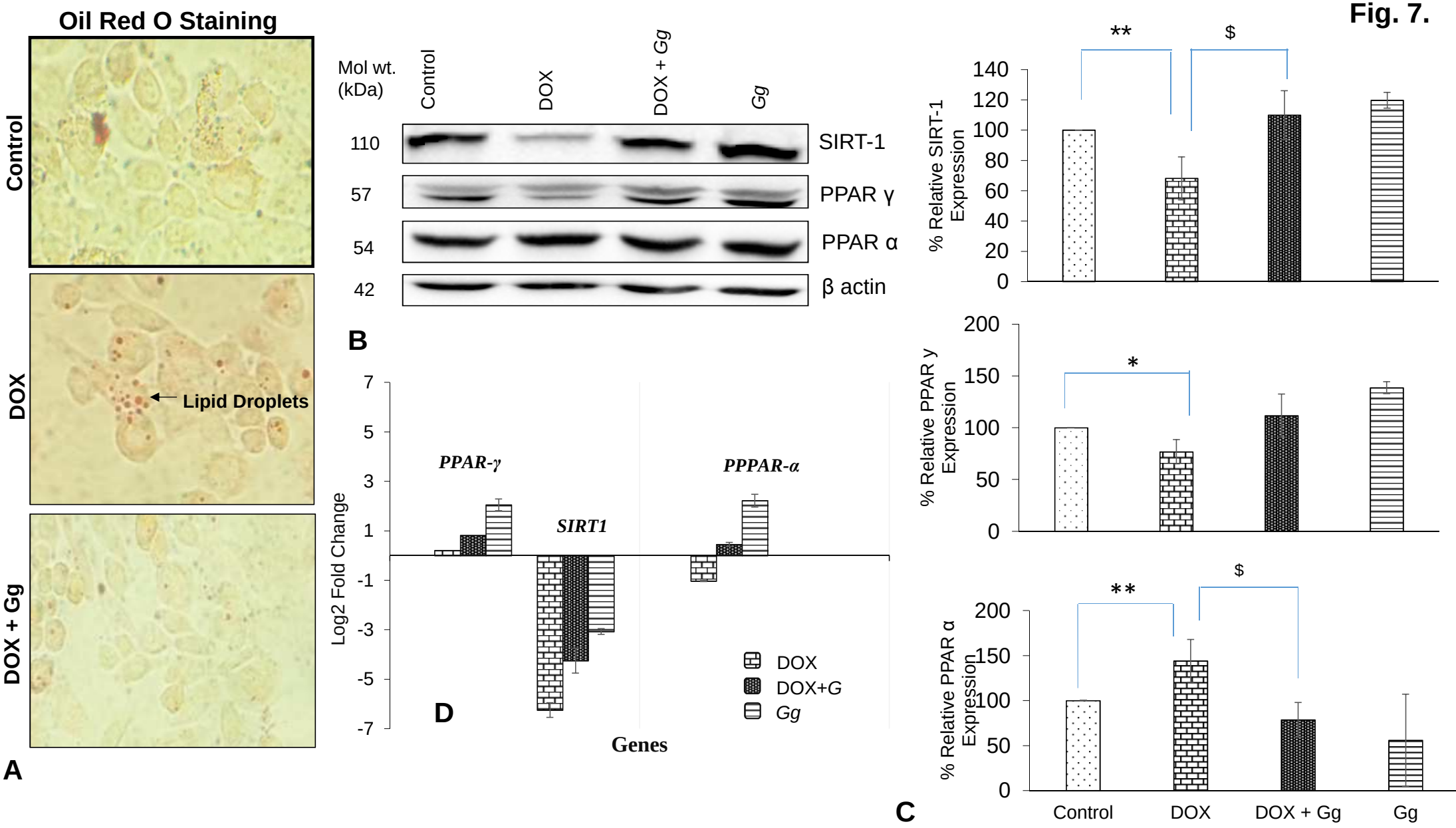
Oil Red O Staining
Control
DOX
DOX + Gg
Lipid Droplets
A
Mol wt. (kDa)
Control
DOX
DOX + Gg
Gg
110
57
54
42
SIRT-1
PPAR γ
PPAR α
β actin
B
Log2 Fold Change
PPAR-γ
SIRT1
PPPAR-α
DOX
DOX+G
Gg
Genes
D
% Relative SIRT-1 Expression
% Relative PPAR γ Expression
% Relative PPAR α Expression
**
$
*
Control
DOX
DOX + Gg
Gg
C

Fig. 8

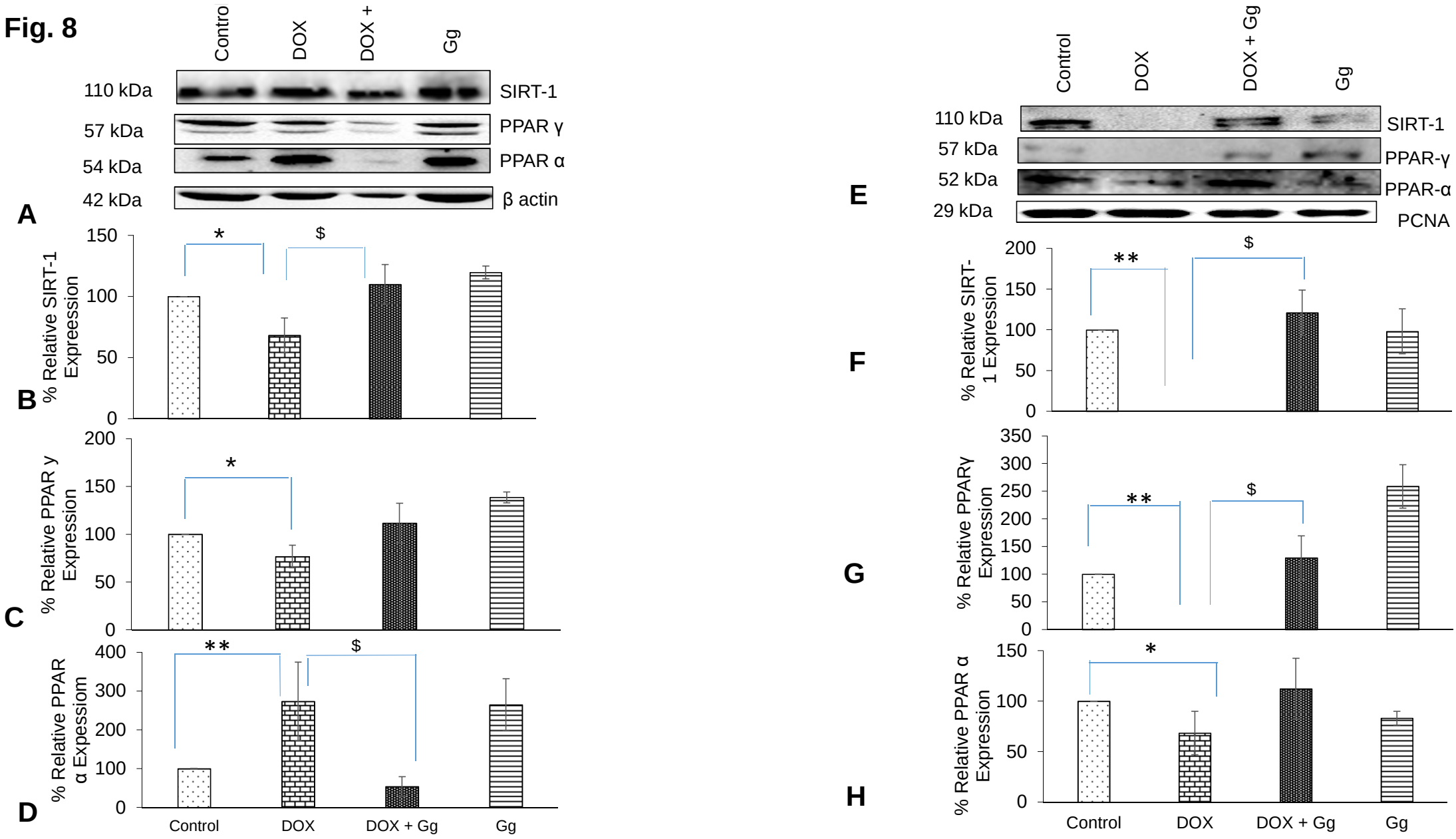
A
Contro
DOX
DOX +
Gg
110 kDa
SIRT-1
57 kDa
PPAR γ
54 kDa
PPAR α
42 kDa
β actin
B
% Relative SIRT-1 Expression
C
% Relative PPAR γ Expression
D
% Relative PPAR α Expression
Control
DOX
DOX + Gg
Gg
E
Control
DOX
DOX + Gg
Gg
110 kDa
SIRT-1
57 kDa
PPAR-γ
52 kDa
PPAR-α
29 kDa
PCNA
F
% Relative SIRT-1 Expression
G
% Relative PPARγ Expression
H
% Relative PPAR α Expression
Control
DOX
DOX + Gg
Gg

Fig. 9

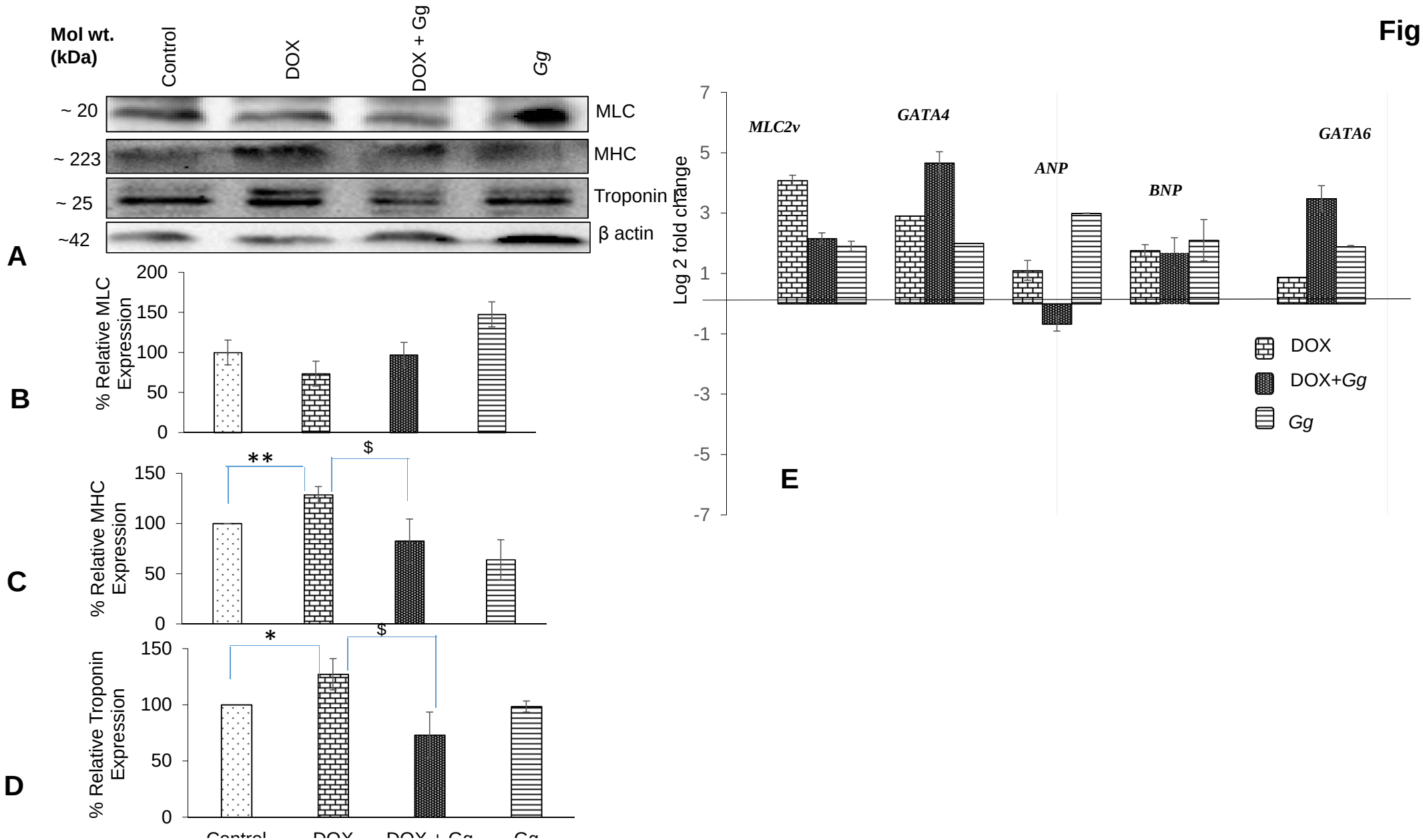
Mol wt. (kDa)
Control
DOX
DOX + Gg
Gg
~ 20
~ 223
~ 25
~42
MLC
MHC
Troponin
β actin
A
B
% Relative MLC Expression
200
150
100
50
0
C
% Relative MHC Expression
**
$
D
% Relative Troponin Expression
*
$
Control
DOX
DOX + Gg
Gg
E
Log 2 fold change
7
5
3
1
-1
-3
-5
-7
MLC2v
GATA4
ANP
BNP
GATA6
DOX
DOX+Gg
Gg

PPAR α Co-Precipitated with SIRT-1

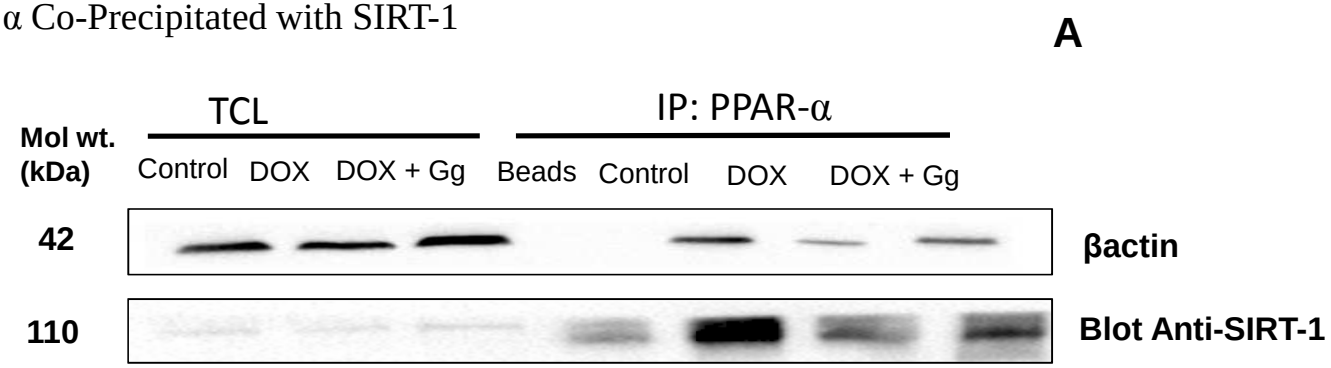

PPAR γ Co-Precipitated with SIRT-1

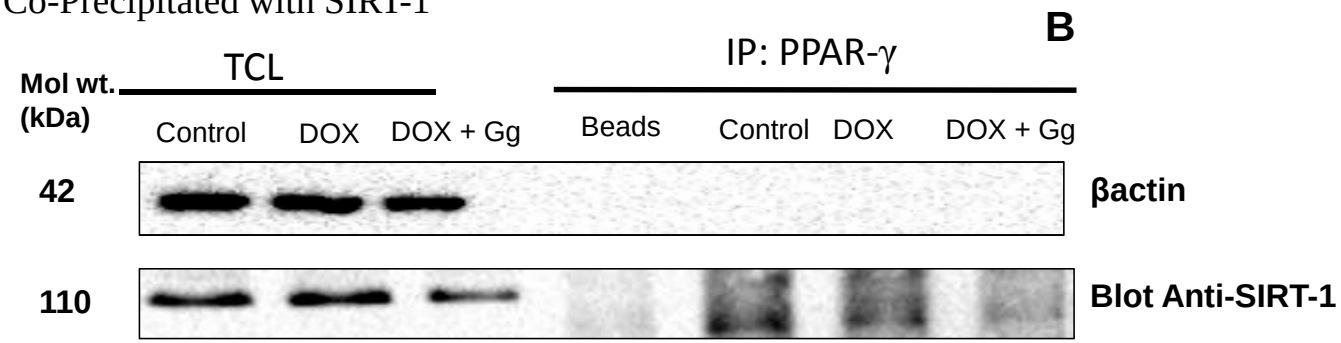

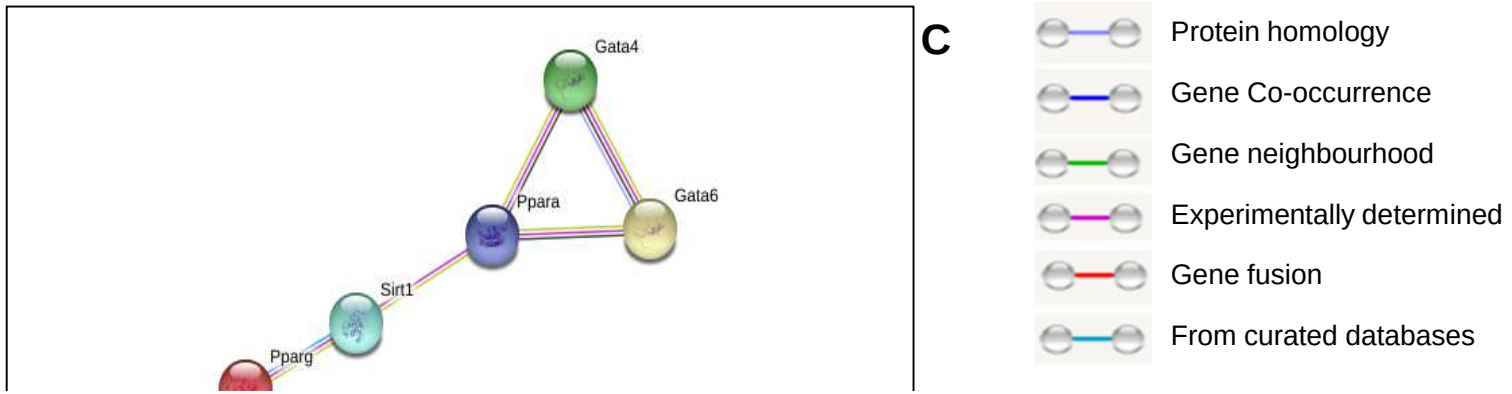

Fig. 10.

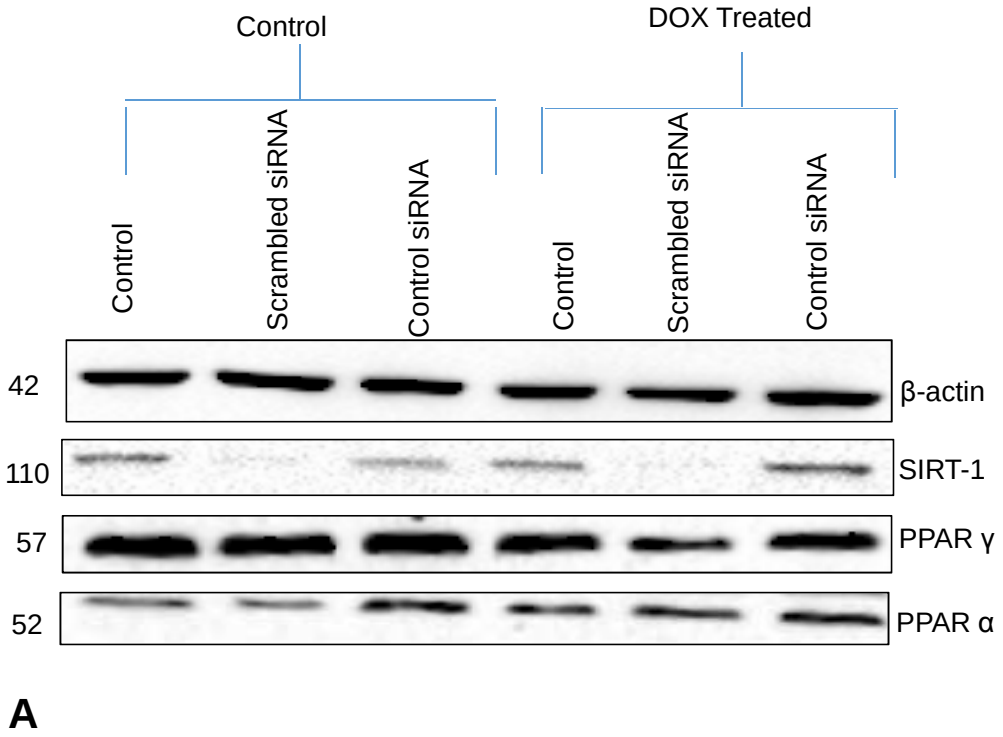
Control
DOX Treated
Control
Scrambled siRNA
Control siRNA
Control
Scrambled siRNA
Control siRNA
42
β-actin
110
SIRT-1
57
PPAR γ
52
PPAR α

A

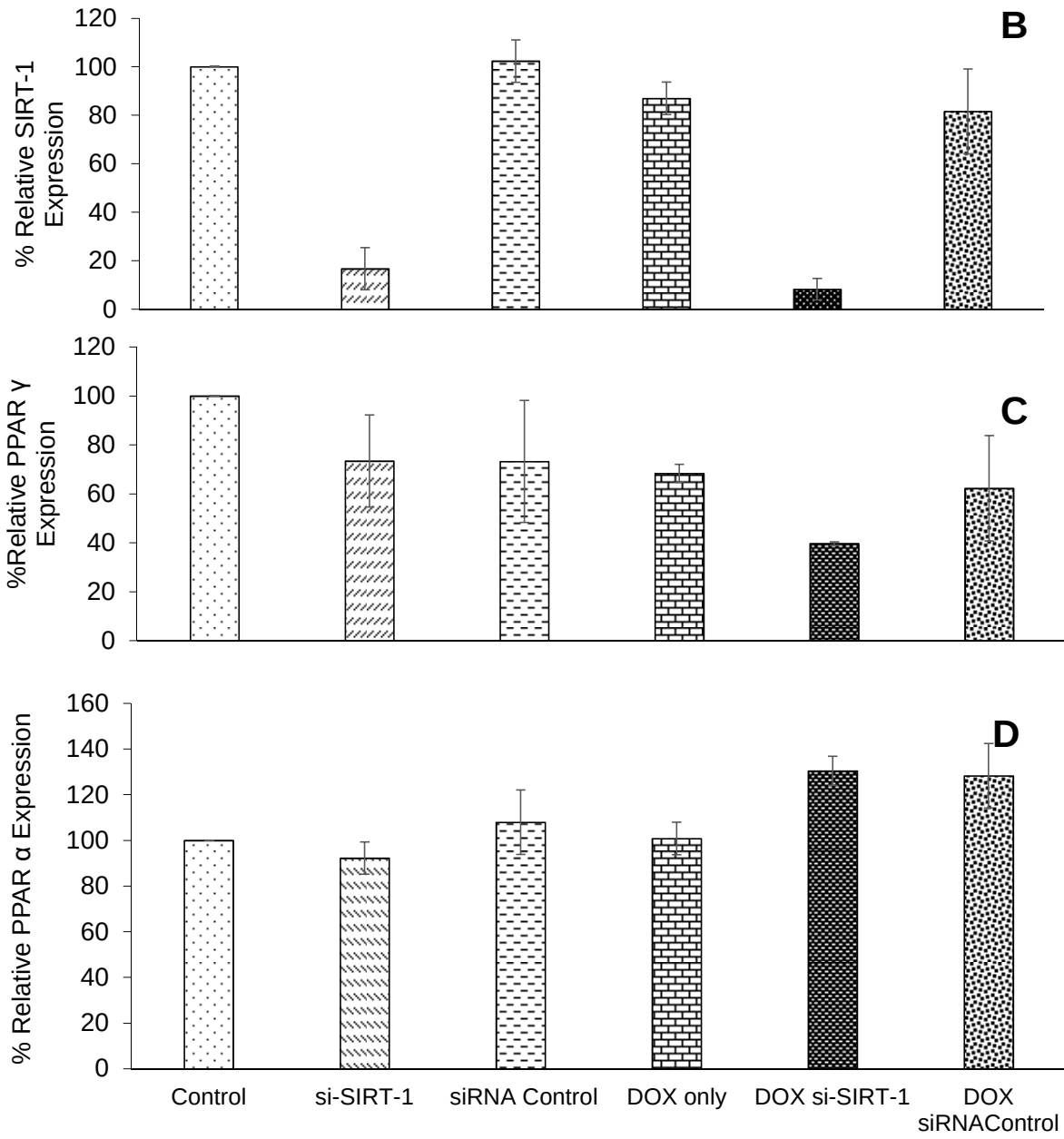
B
% Relative SIRT-1 Expression
120
100
80
60
40
20
0
C
%Relative PPAR γ Expression
D
% Relative PPAR α Expression
160
140
120
100
80
60
40
20
0
Control
si-SIRT-1
siRNA Control
DOX only
DOX si-SIRT-1
DOX siRNAControl

Fig. 11